DYNAMIC RESPONSE ANALYSIS OF TRANSMISSION TOWERS AFTER CONDUCTOR BREAKAGE USING ADINA

JOSEPH I. DUNFORD

DYNAMIC RESPONSE ANALYSIS OF TRANSMISSION TOWERS AFTER CONDUCTOR BREAKAGE USING ADINA

by

© Joseph I. Dunford, P.Eng.

A thesis submitted to the

School of Graduate Studies

in partial fulfillment of the

requirements for the degree of

Master of Engineering

Faculty of Engineering

Memorial University of Newfoundland

April, 2011

St. John's, Newfoundland and Labrador

ABSTRACT

The objective of this research was to (i) assess the peak dynamic and static residual loads on various types of transmission line structures due to conductor rupture, (ii) study the effect of structural flexibility on maximum dynamic impact and static residual conductor loads and (iii) carry out a sensitivity study of various line parameters such as conductor tension, ice load, insulator length and terrain types on the peak dynamic and static residual loads.

To accomplish these objectives, the following tasks were carried out:

- A number of numerical models of a 30 span transmission line were developed and analyzed using the ADINA finite element software package. The initial results were validated by comparing with the full scale test data.
- Four structure types were considered in the detailed analyses. These were: (1) self-supported steel lattice tower with different leg extensions, (2) guyed-V steel lattice tower, (3) tubular steel pole structure and (4) H-frame wood pole structure. The effect of the structures' flexibility on peak dynamic and static residual conductor tensions was studied. after a conductor rupture
- A sensitivity analysis study was conducted to study the effects of various line design parameters such as initial conductor tension, conductor loading (bare conductor, versus loads due to half an inch and one inch radial ice thicknesses) ,insulator length and terrain types (e.g. level, hilly and valley terrains). The results from this study are presented in terms of their effect on impact factors.

The results obtained from the numerical simulation study indicate that the structural flexibility and the span/insulator and the span /sag ratios have considerable effects on the residual conductor tension (hence on the insulator force). However, the peak dynamic tensions are affected not only by the structural flexibility but also by the cross arm mass and the shape of the structures

used for line modeling. For stiff structures, cross arm mass has very little effect on the peak conductor tension. For transmission line modeled with rigid structures, the impact factors are not sensitive to the stiffness values, where as for line modeled with flexible structures, the residual ratio depends on both the stiffness values and span/insulator and span/sag ratios. The effect of insulator string length has more effect on residual ratio than peak impact factor. The specific terrain types that were considered in this study had only minimum effects on the impact factors

KEY WORDS: Broken conductor analysis, Impact factor, Residual ratio, Flexibility correction factor, Residual tension, Peak dynamic force,

ACKNOWLEDGEMENTS

The author of this work would like to gratefully acknowledge the following people for their contributions to this project:

My supervisor, Dr. Katna Munaswamy, for his guidance, encouragement, editing assistance, constructive criticism and wisdom during the pursuit of my Master of Engineering degree, and most importantly for keeping me on track during the course of the research;

Dr. Asim Haldar for editing assistance and guidance throughout the project.

My parents and sister for their support throughout the duration of this work and throughout my life;

My wife Heather and two sons Isaac and Owen for their encouragement, patience, support and most importantly understanding to the end.

TABLE OF CONTENTS

Page

Contents

LIST OF TABLES

Page

LIST OF ILLUSTRATIONS

Page

LIST OF SYMBOLS

ADINA	Automatic Dynamic Incremental Nonlinear Analysis
R_i	Impact ratio
R_r,RR	Residual Ratio
R_o	Tension Overload Factor
IFI	Impact Factor Initial
IFF	Impact Factor Final
LLF	Longitudinal Load Factor
$CF_{S/I}$	Span/Insulator Correction Factor
[C]	Damping Matrix
[K]	Stiffness Matrix
[M]	Mass Matrix
α and β	Rayleigh damping coefficients
ξ	Damping ratio
ω	Natural frequency
RTS	Rated Tensile Strength
C	Structural flexibility correction factor
$1/k_n$	Structural flexibility of N^{th} structure

1.0 INTRODUCTION

Overhead transmission lines are normally designed to withstand two types of loads; primary loads due to ice buildup and wind, and secondary loads, that are dynamic and the less predictable loading due to component failure or ice shedding, galloping, etc.

A large amount of strain energy is stored under heavy loading. In the event of conductor rupture, hardware failure or ice shedding, the sudden release of this stored energy produces dynamic impact loads on the supporting structures along with a high residual longitudinal load. As a consequence of this high longitudinal impact load, the supporting structure can fail that may lead to cascading failures of adjacent structures.

A transmission line can be broken down into three basic components; the support structure, conductors and shield wires, and insulators. There are two broad categories of support structures or towers used in transmission lines; self supported towers and guyed towers. Self supported towers include, steel lattice towers (Figure 1.1), dead-end towers, steel towers, wooden poles, H-frames and other structures that do not require cables or guyed wires to maintain their integrity.

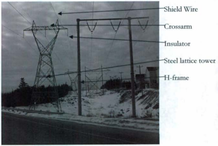

Figure 1.1 Self Supported Towers

Guyed towers (Figure 1.2) require that the tower be pinned at a central point with 4 or more cables/guy wires that anchor and prevent the tower from shifting laterally.

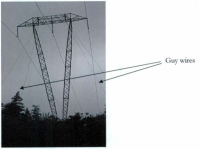

Figure 1.2 Guyed Tower

When ice buildup occurs on a support structure and its conductors, a large static load is applied. This loading is quantifiable and predictable from historical meteorological data. Ice shedding is less predictable given that determining where it will occur on a line and the extent of the shedding, along with a variety of other variables makes it difficult when designing a transmission line. The enormous amount of potential energy that is released at the onset of shedding or component failure can cause a domino effect or cascade failure of a series of towers. The economic loss due to cascade failures is great and is evident in the 1998 lower Ontario and Quebec ice storm that resulted in a cascade of 130 towers and resulted in the single greatest economic catastrophe in Canadian history.

This ice storm saw over 4 million people in lower Ontario, Quebec and New Brunswick lose power. The result was 28 deaths (mostly due to hypothermia), 945 injuries, 130 failed transmission towers (Figure 1.3), more than 30,000 fallen utility poles and cost of over 5.4 billion dollars.

Figure 1.3 Severe Ice Loading on Conductors during the 1998 Ice Storm

A more recent and local event occurred on a section of line owned by Newfoundland Hydro during the winter of 2010. This system or string was comprised mainly of wooden pole and H-frame structures that were compromised when an ice storm moved into the Bonavista region and moved towards Trinity. The storm began on a Friday evening and lasted into the weekend. The result was over 100 fallen poles and about 7000 homes without power for 4 days. Crews worked around the clock for 4 days before power was restored to all areas. A glimpse of the severity of that storm can be seen in Figure 1.4 and Figure 1.5.

Figure 1.4 Fallen H-frame during the Bonavista-Trinity Ice Storm of 2010

Figure 1.5 shows the severity of ice loading on the conductors during the Bonavista storm with loading in the range of 1.5 to 2 inches radial thickness.

Figure 1.5 Ice Loaded Wooden Pole line during the Bonavista-Trinity Ice Storm of 2010

There are three potential cascades that can occur: vertical, transverse and longitudinal. A vertical cascade occurs when a piece of hardware, section of the cross arm, or insulator fails that causes the conductor to fall vertically over a series of support structures. A transverse cascade can occur when there is wind that is perpendicular to the transmission line. If a component (such as a guy wire) fails that causes a cascade where the conductor falls perpendicular to the direction of electrical transmission or the tower can be seen to fall perpendicular to the conductor wire. A longitudinal cascade is when a tower fails parallel to the conductor wire (see Figure 1.6).

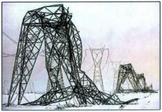

Figure 1.6 Failed Transmission Towers of 1998 Ontario-Quebec Ice Storm

The longitudinal cascade is the most common and most destructive of the three and as a result most research & development has been focused on preventing of minimizing this type of failure. Primary causes for the initial tower failure can be longitudinal imbalance, uneven ice, wind or broken conductors (Thomas and Peyrot [8]). The most common method of cascade prevention currently is to insert cascade arresting towers or dead-end towers. The difference between a dead-end tower (see Figure 1.7) and the standard support structure is that these are designed to withstand a higher longitudinal load. These are usually inserted at regular intervals or at critical points in the distribution network. The disadvantage of this solution is that this can be costly as these towers are much more robust. Another method that is employed is the use of impact factors (Thomas and Peyrot [8]) when designing a tower. Therefore if a more complete knowledge base of dynamic responses were available then this could be used in transmission line design to limit cascading to a few towers or none, hence reduce costs and improve system reliability.

Figure 1.7 Dead end tower

The purpose of this research is to develop a greater understanding of the dynamic response of a transmission line immediately following a rupture, using commercially available computer simulation software.

1.1 Scope

Overhead lines are normally designed to withstand two types of loads; primary loads arising from direct meteorological exposures, such as ice and wind, and secondary loads, often known as the unbalanced loads due to ice shedding, or the failure of a component such as conductor, hardware etc. Primary loads are typically specified by a design return period, and are usually applied as maximum ice, maximum wind, and some combination of wind and ice. The design return period is selected by balancing the initial capital cost of building the line against the cost of failure (damage) during its lifetime operation. Also, the importance of the line plays a significant role in selecting the design return period. Radial lines are typically more critical than parallel lines or lines within a grid as failure of a radial line often causes an extended outage to the customer

Due to the large amount of stored energy under heavy loading, failure of mechanical components in the system, such as insulators or dead-end hardware, can produce significantly large dynamic loads that are difficult to quantify or to design for. These dynamic secondary loads, even when the primary loads are less than the design load, can far exceed the structure capacity and can trigger a failure event in the system. A large amount of energy released can cause catastrophic failures

A better understanding of the dynamic loads experienced during cascade failure would provide designers with the tools required to cost effectively and reliably design the transmission systems and to minimize damage from single component failure. This is especially important when consideration is made for the premature failure of a component below the design load level, which can cause a cascade that could otherwise be prevented or minimized with a proper design methodology. There is a strong need to understand the post failure force distribution in a line.

Over the course of 30 years, work has been completed on the dynamic response of transmission line failures. The research has involved 3 types of analysis; full scale, reduced scale experimental testing, and computer simulation using analysis software such as ADINA (Automatic Dynamic Incremental Nonlinear Analysis). Until recently, the extent of simulation analysis has been limited; however it has been shown in previous work (Tucker and Haldar [1]) that the ADINA software can be used to simulate conductor breaks in the transmission line to obtain comparable results to the full scale test data.

1.1.1 Objective of the Project and Scope

The present study uses a hypothetical 230kV steel line configuration with 30 structures. The 230 kV line consists of a single circuit horizontal configuration. Also a wood pole line as well as a steel tubular pole line is considered at this voltage level to assess the effect of structure's flexibility on the containment loads. Three different structure types are considered. These are (1) latticed self supported tower with different extension legs (2) Guyed-V tower, (3) tubular steel pole structure and (4) wood pole H-frame structure.

The objectives of this study are:

- to assess the peak dynamic and static residual loads on these structure types due to conductor rupture
- to study the effect of flexibility of supporting structure in the transmission line on maximum dynamic impact and residual conductor loads.
- to carry out a sensitivity study of various parameters such as (1) conductor tension, (2) ice load, (3) insulator string length and (4) terrain on the peak dynamic and static residual loads.

To accomplish these objectives, the numerical model of the transmission line that was developed was analyzed using ADINA finite element software package and validated by comparing with the full scale experimental data.

1.2 Thesis Organization

Chapter 2 is a summary of work that is relevant to the current research. It describes work that has been conducted over the last century to further our understanding of the dynamic response that results from a conductor or tower failure.

Chapter 3 explains some of the parameters that are considered when performing a simulation. This chapter involves simulations of the EPRI Wisconsin Test Line and compares the actual results with the simulated results. This was performed as a validation of the assumptions used for the current research.

Chapter 4 discusses the modeling considerations when using the ADINA software and the variables, assumptions and methodology involved when modeling the various towers in a transmission line. Material properties for the various components used throughout this research are given in this chapter.

Chapter 5 investigates the free vibrations of the towers and conductors and their effect on the Rayleigh damping coefficient used in the analysis.

Chapter 6 explores the methodology involved when performing a dynamic analysis. This chapter also examines the span/sag ratio, tower structural flexibility and their affects on peak conductor tension. In addition, variable cross arm mass for the flexible wooden H-frame structure was examined for its affects on dynamic peak load with the use of the three impact factors IFF, IFI and RR.

Chapter 7 presents a sensitivity analysis of tower type, insulator length, terrain type, initial conductor tension, conductor loading and provides a discussion there into.

Chapter 8 summarizes and discusses the findings of this research.

Chapter 9 identifies topics for further research.

2.0 LITERATURE REVIEW

The first transmission of electricity from a generating plant in Frankfurt to Lauffen, in Germany occurred in 1891. The power was transmitted over a 175km line operated at a 25kV level. By 1914, fifty five transmission lines were in service at or above 70kV level. Although the high voltage line design uses various structure types due to voltage differences, there are a few commonalities that must be considered in the design process: selection of an optimum conductor size, meteorological loads and their effects, analysis and design of structures and foundations etc. In recent years, the focus of the research has been to estimate the dynamic loads on overhead line structures caused by a component failure. The review of literature is broken down into three parts. Each part describes the research work carried out during a specific period

2.1 Significant Research Work Prior to 1980

After the Second World War, a considerable research effort was directed to establish safe design requirements for transmission towers. From 1950 to 1980 the focus of research was on the broken conductor testing of the decommissioned transmission lines to estimate peak dynamic and residual loads on the supporting structures. In addition, much attention was paid to the mathematical modeling of transmission lines and the development of dynamic impact factors.

Haro et al [2] conducted a series of full-scale tests where they examined the dynamic peak force acting on the supporting structure due to a conductor breakage. The sensitivity study included the effects of flexible and rigid towers, initial conductor tension, insulator lengths and the various cross sectional areas of conductor on the dynamic and static residual loads. They observed that immediately after the conductor rupture, the force in the conductor decreased up to a value of 95% of the initial tension. This reduction was followed by a sharp increase in the conductor tension. The elapsed time from the initiation of the rupture to the time where the tension again began to rise was termed as the "slack" time. It was also observed that this "slack" time was directly proportional to the length of the insulator. The peak dynamic force increases with the increase in initial conductor tension. The ratio of the peak dynamic force to the initial conductor tension decreased with the increase in initial tension. It was also observed that the peak dynamic force in the conductor decreases with the increase in insulator length. In addition, the flexible structures experienced a peak load which was two thirds of the load on the rigid structures.

Lummis et al [3] developed a mathematical model to study the effects of structural flexibility on the unbalanced loading imposed by the conductor rupture. A graphical method was used to determine the unbalanced longitudinal load on the structure by adjusting the conductor tension based on an increase or decrease of unstressed length (USL) effect on the tension. It was pointed out that the inherent flexibility of the tubular steel pole structure will provide economical design because the loads on the structure will be reduced significantly. The paper also identified the need for a computer aided analysis method as opposed to a graphical approach to reduce the analysis time.

Govers [4] carried out a number of dynamic tests on small scale line models in the laboratory and full scale field tests on a decommissioned line. The author used three impact factor ratios for comparison of these tests namely, Impact Ratio (R_i), Residual Ratio (R_r), and Tension Overload Factor (R_o). These ratios are defined as follows.

$$R_i = \frac{\text{Dynamic transient peak of longitudinal force}}{\text{Initial static force of conductor}}$$

$$R_r = \frac{\text{Residual static force}}{\text{Initial static force of conductor}}$$

$$R_o = \frac{\text{Dynamic transient peak of longitudinal force}}{\text{Residual static force}}$$

Where the dynamic transient peak longitudinal force is defined as the maximum force induced in the conductor due to the conductor rupture, the initial static force of conductor is defined as the force in the conductor prior to the conductor rupture and the residual static force is defined as the force in the conductor after the conductors reaches equilibrium condition after the rupture. These ratios were found to be directly affected by the span/sag ratio and the span/insulator ratio. Govers concluded that increase in the span/sag and span/insulator ratios produced a decrease in the impact ratio (R_i). The impact ratio showed a significant reduction when the inverted V shaped insulators were used compared to that obtained using regular suspension string insulators.

Peyrot et al [5] conducted a series of tests involving broken conductors, shield wires and insulators on a decommissioned double circuit 138 kV line. The test line consisted of six spans. All of the supporting structures were self supported steel lattice towers. It was reported that immediately following a conductor rupture, the tension in the insulator string almost reduced to zero for a short period of time and then showed a steady increase until the first peak force in the insulator string was realized. Following this rise, the force in the insulator string dropped again and then the force increased again to a higher peak. From these full scale tests, the authors calculated two impact factors. These were: Impact Factor Initial (IFI) and Impact Factor Final (IFF). These impact factors were similar to those suggested by Govers [4].

Lindsey [6] conducted a static analysis to determine the residual load in the conductor. In this study, the base support for the structure was modeled as elastic-plastic. Prior to this study, the base support was modeled as elastic or rigid. The author used "Southwell Relaxation Method`` to solve the nonlinear system of equilibrium equations which included the effects of structure's deflection and the insulator swing after the conductor rupture

2.2 Significant Work From 1980 – 1989

Most of the research work from this era identified the need for modeling the dynamic response of transmission lines and the development of algorithms that formed the basis for simulation programs.

Mozer et al [7] conducted a series of tests on small scale ($1/30^{th}$ scale) line models with three equal spans to obtain static and dynamic data on the longitudinal loadings and structure responses due to broken conductors, broken shield wires or ice shedding conditions. These laboratory scale models were constructed using beaded chain and copper wires with lead shot weights to simulate the proper mass characteristics. The effects of stiffness, initial conductor tension, insulator length etc. on the peak dynamic force were studied. The test results were compared with the theoretical results. From the results they concluded that the dynamic loads and structure response effects resulting from the broken conductor in the line will often be quite large. It may not be feasible to design the tangent structures to sustain these loads without yielding. However, they may serve as indicators of potential structural problems rather than as loads to be presented as design specifications.

Thomas and Peyrot [8] discussed the need to quantify the force time history after a conductor rupture. The objective was to capture the accurate peak dynamic load on the tower to ensure that the estimated load will provide a measure of the containment load that is needed to avoid a cascade failure. Until this time, the design process was to use typical impact factors to estimate the longitudinal loads on the tower. The authors developed a wave propagation model that is used in further research and computer modelling. A graph of the time history of a dynamic response of conductor showed a double peak with the second peak being the maximum tension experienced in the line after a conductor rupture. This peak tension occurred within a couple seconds after the conductor failure. They identified the time between the drop in tension near to zero to the point where one observes the first peak as *slack time*. They described that the first peak occurs due to the recoil of the insulator swing. The second peak occurred when the cable bottoms down. The authors used the FORTRAN based program CABLE7 to simulate a dynamic response. They verified their simulation results with Ferry-Borges small scale study [24].

Richardson [9] used a $1/25^{th}$ scale model of a steel pole system consisting of eleven spans to carry out broken conductor tests and to measure the dynamic loads on the pole structures Richardson found that the use of more flexible structures will minimize the maximum dynamic load of the system as compared to rigid structures. In addition it was identified that when a break occurs at the most flexible structure then the dynamic load increases but ice shedding produces the greatest dynamic response when it occurs at the most rigid structure. Higher dynamic responses occurred when a longer insulator was used due to a higher galloping affect of the conductor. From the testing it was found that longer insulators and stiffer structures contributed to a higher peak load.

McClure and Tinawi [10] performed broken conductor nonlinear dynamic analyses of a small scale model of a transmission line section using ADINA and compared the numerical results from this study with the experimental results reported by Mozer et al. [7]. They reported that the higher frequency components of the response from the numerical results must be filtered in order to achieve numerical stability. The authors explained the importance of accounting for nonlinearities in the structure and conductors. They also identified the need to properly model the base of the structure. They did not consider damping; however the results showed a strong correlation between the simulated results and the small scale test results. They identified the need to properly model the base of the structure.

2.3 Significant Work from 1990 - Present

During the past twenty years, the research work has primarily focused on the numerical modeling of transmission line system with particular reference to predicting the peak dynamic loads on the structure after a component failure

Jamaleddine et al [11] conducted a series of laboratory tests on two span reduced-scale setup representing two level equal spans anchored at the end points and suspended in the middle by insulator string. They simulated ice-shedding loads by suddenly dropping dead weights from the conductors. They also used ADINA to develop numerical model to obtain the static dynamic response of the line model. The numerical results were compared with the experimental data. The numerical results for tensions were similar to the measured values but peak dynamic tensions were higher than the experimental data.

Gupta et al [12] carried out a detailed analysis of a real life cascade failure of 69 towers of a 345kV transmission line that occurred on March 7, 1990 due to a severe ice storm. The ice storm produced an ice thickness between 1.25-1.5 inches accompanied by an average wind speed of 12.1 mph. The authors used the FEA (Finite Element Analysis) software ETADS to simulate the nonlinear analysis.

Ostendorp [13] developed a cascading failure risk assessment method to quickly and accurately determine extreme event unbalanced loads acting on a transmission line and to identify cascading potential of a line. The method developed incorporates the dynamic response and damping characteristics of transmission line to determine the unbalanced longitudinal loads at any structure rather than unbalanced load acting on the first structure from the initiating event.

Kempner [14] conducted small scale model (1/23 scale) tests to understand the influence of the tower failures on the longitudinal load in a simulated cascading situation. The influence of tower type, conductor type, span length initial conductor tension and insulator lengths on longitudinal cascading failure were studied.

Fekr and McClure [15] studied the dynamic effects of ice-shedding on a transmission lines using a numerical model. They modeled a two span line section to obtain static and dynamic effects of ice-shedding using ADINA software. A total of twenty one ice-shedding scenarios were studied; varying ice thicknesses; span lengths; elevation differences; number of elements per line; presence of unequal spans and partial ice shedding.

Peabody and McClure [16] discussed use of cascade prevention devices to limit the dynamic forces on tangent suspension towers after an initial failure in the cable tensioning system. They have reviewed the development and use of load limiters for transmission towers

McClure and Lapointe [17] discussed three types of analysis techniques to simulate the behavior of transmission lines. These were described as, (i) static behavior under ice loading, (ii) quasi-static behavior under wind loading and (iii) dynamic/transient behavior – due to sudden failure of component or shedding of ice. Damping was modeled using viscous dampers in ADINA. The damping ratios of 2% for bare cables/conductors and10% for iced cables/conductors were used. The authors compared the results from 2-D and 3-D analyses. It is noted that when a 3-D modeling system is used "…it is seen that the first and second peak tensions in the three-dimensional model are delayed with respect to the two-dimensional model and also have a longer duration."

Tucker and Haldar [1] carried out a sensitivity analysis of a line model to simulate the broken insulator failure test that was conducted on a full scale test transmission line. A numerical model was developed using the ADINA software to simulate the broken insulator test conducted by Peyrot et al [5]. The numerical results were compared to the test data and the correlation of the plot was 0.9776. The results showed that the variation in the insulator length did not influence the peak dynamic load.

2.4 Summary of Previous Work

Much research has been undertaken over the last 60 years to advance the design and analysis of transmission distributions systems. It started with static analysis, scaled tests and full-scale which then progressed to linear elastic flexible steel poles and now using 3-D non-linear analysis using Finite Element software programs such as PLS-CADD, PLS-POLE, TOWER, ANSYS and ADINA. The accuracy of response analyses using these programs is improving. The simulation studies to date have considered a small number of simulations without consistency between studies. There is a need for a single large scale study of key design parameters with consistent simulation methods to add to the current knowledge base.

3.0 VALIDATION OF MATHEMATICAL MODEL USING ADINA

In 1978, The University of Wisconsin and the Electric Power Research Institute (EPRI) carried out a series of full-scale broken conductor and broken insulator tests on one section of a 138 kV steel transmission line. The line was part of the Wisconsin Light and Power' system and was ready for replacement. These tests were performed to advance the state of the art at that time and to verify the containment load prediction techniques in line design, and to validate customized numerical models (Thomas, [8]) as alternatives to laboratory scale model or full-scale testing. The report (EL-905) is one of the few that provides a very comprehensive set of full scale test data and results complete with all necessary information required for subsequent analysis and modeling.

In the present study, the Wisconsin test line was chosen to validate the numerical model. The profile of the test line is shown in Figure 3.1. Six intact spans were included in the modeling; with all structures being square based lattice steel towers, each tower carrying two three-phase circuits, each circuit strung with different conductor types, and two overhead shield wires. Figure 3.2 presents the geometry and the member types that were used in modeling the tower. The data on the conductor attachment points were used as given in Ref [5]. The line angle of the original test line between Tower T4 and T6 was not considered in the model. The assumption was that this small deviation of transmission line may not have significant effects on the results. Anchor ground points for the conductors were chosen to be at fifty meters (50 m) from the two end towers.

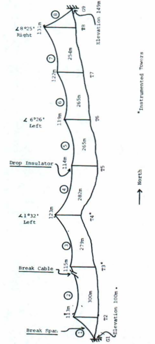

Figure 3.1 EPRI Wisconsin test line [5]

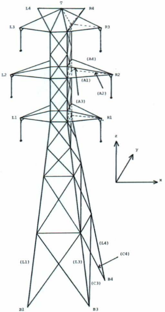

Figure 3.2 EPRI Typical tangent tower [5]

3.1 Modeling in ADINA

The general outline for transient response analysis in ADINA requires the development of a finite element (FE) model of the line followed by a static run to ensure that the initial position of the cable geometry under gravity load (self weight) was captured. A routine check on the sag and the tension provides the basis for assuming that the model is correct with respect to initial tension, axial rigidity (EA) and the boundary conditions. The detailed methodology for modeling overhead lines using ADINA is given in CEATI report no. T043700-3319A (2006) and in Tucker (2007). The following provides the highlights of the procedure that was used in the present study to develop an ADINA model.

- The conductor and the shield wire are modeled as truss elements with initial pretension.
- The conductor material can be modeled as elastic (final modulus) or non linear elastic (initial modulus).
- The tower is modeled as a linear elastic beam element with appropriate equivalent stiffness. For a "stick" model however, if the model includes the full tower then three dimensional truss elements are normally used.
- The load is defined as mass proportional.
- The static model is run first; the result is saved and used as the restart condition for the transient dynamic analysis.
- Direct explicit integration technique is used to solve the equations of motion. The time step is less than a critical time step, which depends on the smallest element size and material properties. The time step can be

specified by the user or calculated automatically by ADINA. It was found that time step is less than 1 E-04 second in all cases.

- The static model part is initialized at 1.0 second and the cable "death" element (element removed from the model to simulate a broken conductor) is activated at 1.001 second to simulate the conductor break.

Once the static analysis is completed, the transient response analysis is carried out by invoking the "element death" option in ADINA which allows the simulation of a cable rupture at any location. When the element death option is used, the program does not add the associated element mass matrix, stiffness matrix and load vectors to the system matrices for all solution times larger than the time of death of the element, t_{Death}. For details refer to the ADINA manual (Section 10.4, pages 593-602).

When the cable element "dies", the insulator at the break point, as well as insulators in the other spans, is free to swing fully. A step by step time step integration of the equations of motion of the discrete system provides the time history responses of various parameters such as displacement, conductor tension, force in the insulator string, etc. ADINA does not provide the insulator swing directly but this can be computed using the two displacement components (y- and z-) at the top and bottom nodes of the insulator element.

- The size of the output file from a typical dynamic analysis run is very large. The output file (Port file in ADINA) can be saved at specific time intervals to reduce the size of the file. The post processing of the output file provides the time history plots of element forces, nodal displacements, stresses and strains in the element, etc.

3.2 Static Test Results (Tower only)

The tower responses e.g., member forces due to static loads applied at the right lower arm (R1 in Figure 3.2) in Y and Z directions and the loads applied at the top of the tower (T in Figure 3.2) in Y direction were analyzed. Table 3.1 compares the predicted responses with those reported in Ref [5] and the results are in good agreement.

3.3 Natural Frequencies and Mode Shapes of the Tower

Free vibration analysis of the tower was carried out to obtain the natural frequencies and mode shapes. The natural frequencies obtained from the analysis are given in Table 3.2. The first five mode shapes along with their frequencies are shown in Figures 3.3 and 3.4. The damped natural frequency of the tower in the longitudinal direction (bending mode) was reported as 4 Hz in Ref [5]. The numerical value of

4.62 Hz obtained in the present work, compares well with the test result reported in Ref [5] with an error margin of 15%.

Table 3.1 Analytical Static Test Results

(Values in brackets are from Ref[5])

		T	R1	
		Y	Y	Z
Reactions (Kgf)	B1 X	-404.8 (-403)	-428.4 (-414)	39.13 (41)
	B1 Y	-254.6 (-251)	-101.01 (-91)	19.70 (-17)
	B1 Z	-2439.03 (-2367)	-1609.27 (-1516)	-92.52 (-78)
	B2 X	398.61 (403)	63.6 (82)	-41.58 (-41)
	B2 Y	-247.03 (-251)	-403.18 (-412)	99.85 (100)
	B2 Z	-2403.08 (-2367)	-1443.36 (-1467)	592.5 (578)
	B3 X	-398.87 (-403)	-64.36 (-82)	-39.13 (-41)
	B3 Y	-246.8 (-251)	-403.09 (-412)	-97.40 (-100)
	B3 Z	2403.08 (2369)	1443.36 (1467)	578.53 (578)
	B4 X	405.57 (403)	429.1 (414)	41.58 (41)
	B4 Y	-251.5 (-251)	-92.718 (-89)	17.25 (17)
	B4 Z	2439.03 (2367)	1609.27 (1516)	-78.53 (-78)
Forces in Base Members	L1	2315.27 (2284)	1366.2 (1328)	163.8 (151)
	L2	2288.00 (2284)	1239.0 (1269)	-594.48 (-588)
	L3	-2287.61 (-2284)	-1238.0 (-1269)	-583.12 (-588)
	L4	-2319.6 (-2284)	-1379.1 (-1328)	152.45 (151)
Deflection at Load points (cm)		1.91238 (1.902)	0.96099 (0.9732)	0.49257 (-0.4961)

Table 3.2 Tower Natural Frequencies

Mode number	Frequency (Hz)	Natural Frequency(rad/sec)
1	4.5308E+00	2.8468E+01
2	4.6273E+00	2.9074E+01
3	7.9666E+00	5.0055E+01
4	1.1643E+01	7.3158E+01
5	1.1851E+01	7.4462E+01
6	2.0888E+01	1.3125E+02
7	2.1139E+01	1.3282E+02
8	2.2140E+01	1.3911E+02
9	2.4515E+01	1.5403E+02
10	2.4953E+01	1.5679E+02
11	2.7319E+01	1.7165E+02
12	2.9265E+01	1.8388E+02
13	3.1998E+01	2.0105E+02
14	3.2597E+01	2.0481E+02
15	3.4440E+01	2.1639E+02
16	3.5876E+01	2.2541E+02
17	3.7023E+01	2.3262E+02
18	4.0400E+01	2.5384E+02
19	4.5543E+01	2.8616E+02
20	4.8160E+01	3.0260E+02

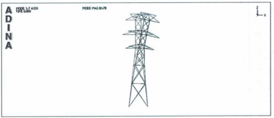

Figure 3.3 First Bending Mode (4.5308 Hz)

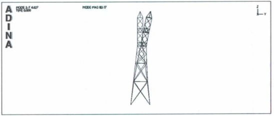

Figure 3.4 Second Bending Mode (4.6273 Hz)

3.4 Natural Frequencies and Mode Shapes of the Test Line

The numerical models of the tower along with the transmission line are shown in Figures 3.5 and 3.6. Free vibration analysis of the test line was conducted to obtain the natural frequencies and the mode shapes. The initial tensions reported in Ref [5] were used to model the conductors and the shield wires. The natural frequencies of the test line are presented in Table 3.3. The first twenty nine (29) frequencies are due to swaying mode of the conductors (transverse displacement mode of the conductor). Only the vibration modes corresponding to the heave modes (vertical displacement mode) participate in the transient response due to the conductor rupture. These modes are identified by examining the mode shapes. The frequencies presented in bold letters correspond to conductor's heave modes. These mode shapes are presented in Figure 3.7. The natural frequencies associated with heave mode are within the expected range.

Table 3.3 Natural frequencies of the test transmission line

(Bold values correspond to conductor vertical displacement modes)

Mode Number	Frequency (rad/sec)	Natural Frequency (Hz)
1	3.247E-02	2.040E-01
2	3.260E-02	2.048E-01
3	3.285E-02	2.064E-01
4	3.599E-02	2.261E-01
5	3.898E-02	2.449E-01
6	4.270E-02	2.683E-01
7	6.496E-02	4.081E-01
8	6.522E-02	4.098E-01
9	6.572E-02	4.129E-01
10	7.201E-02	4.525E-01
11	7.798E-02	4.900E-01
12	8.543E-02	5.367E-01
13	9.742E-02	6.121E-01
14	9.777E-02	6.143E-01
15	9.857E-02	6.193E-01
16	1.080E-01	6.786E-01
17	1.169E-01	7.345E-01
18	1.281E-01	8.046E-01
19	1.299E-01	8.161E-01
20	1.302E-01	8.183E-01
21	1.314E-01	8.257E-01
22	1.440E-01	9.047E-01
23	1.557E-01	9.785E-01
24	1.631E-01	1.025E+00
25	1.636E-01	1.028E+00
26	1.650E-01	1.037E+00
27	1.706E-01	1.072E+00
28	1.808E-01	1.136E+00
29	1.957E-01	1.229E+00
30**	**1.983E-01**	**1.246E+00**
31	1.988E-01	1.249E+00
32**	**2.008E-01**	**1.262E+00**
33	2.011E-01	1.263E+00
34	2.011E-01	1.264E+00
35**	**2.033E-01**	**1.277E+00**
36	2.045E-01	1.285E+00
37	2.058E-01	1.293E+00
38	2.096E-01	1.317E+00
39	2.134E-01	1.341E+00
40	2.143E-01	1.347E+00

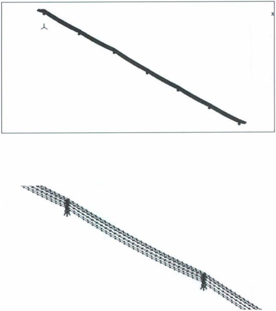

Figure 3.5 EPRI Wisconsin test line model close up view between two towers

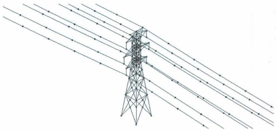

Figure 3.6 Magnified view of the model

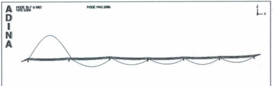

First vertical vibration mode of test line (0.198318 Hz)

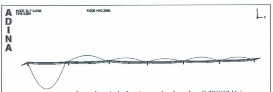

Second vertical vibration mode of test line (0.200822 Hz)

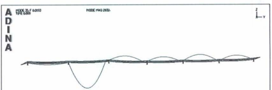

Third vertical vibration mode of test line (0.203254 Hz)

Figure 3.7 Vertical displacement mode shapes of complete test line

3.5 Broken Conductor Tests Sequence

Full scale tests [8] on the test line were conducted in a particular sequence. The video of the full scale tests also confirmed the test sequence. The sequence is as follows.

I. Free vibration of tower

II. Broken Insulator tests

R.1 Right side, lower phase

R.2 Right side, middle phase

L.1 Left side, lower phase

L.2 Left side, middle phase

III Broken Conductor tests

R.1 Right side, lower phase

R.1.a (Conductor slipped through clamp)

R.2 Right side, middle phase

R.3 Right side, upper phase (arm broke)

R.4 Right side, OHGW

L.1 Left side, lower phase

L.2 Left side, middle phase

L.3 Left side, upper phase

IV Broken Insulator tests (Longer insulator lengths)

R.1 through L.2 same as in II above

V Broken conductor tests (Longer Insulator lengths)

VI Sever all cables between G1 and T2.

In this study, the numerical analyses were carried out corresponding to test numbers IIIR1 through IIIL3. .

3.6 Methodology-Static and Dynamic Analyses

3.6.1 Initial Static Analysis.

A static analysis is first carried out using mass proportional loading. The mass proportional loading is defined as the gravity loads acting on the elements. Once the static analysis with mass proportional loading is completed, the line system will be in static equilibrium. The tension predicted from the ADINA model run was close to the initial conductor tension used in generating the sag profile. The predicted force in the insulator string is also close to the lumped weight of the conductor for a full span. The ADINA software saves the static analysis results in a file along with a restart option for subsequent analysis. The file contains the system configuration, element deformations (displacements, forces etc.) and stress/strain data necessary for restart analysis. Restart data from the static analysis is saved only for the last one second.

3.6.2 Dynamic Analysis and Simulation of Conductor Break

The dynamic analysis is carried out using the restart option. Before starting the dynamic analysis, some of the system parameters can be changed in the data input file such as material density, damping properties, death elements etc. The line configuration data and the cross sectional properties of the elements cannot be changed. The break in the conductor is simulated by invoking the 'death element' option in ADINA. The rupture in the element is initiated at time 1.001 sec. The dynamic analysis was performed using explicit direct integration methods.

3.6.3 Simulation of Ice Load on the Conductors

Simulation of ice load on the conductor is done by changing the density for the conductors. After the initial static analysis is completed, the conductor's mass density is modified to simulate the weight of the radial ice. The element mass matrices and conductor loads are calculated with the modified mass density and the original cross sectional area of the conductor. A second static analysis is performed to obtain the new static equilibrium of the line system with radial ice on the conductor. This analysis is done using a restart option and starts from the previous equilibrium condition obtained under bare conductor scenario. With this restart analysis, the sag and conductor tension are increased due to the effect of the ice loads. After the completion of the static analysis under ice loads, the restart data file is saved for one additional second, thus providing information for a total of two seconds. The first one second information refers to bare conductor while the last one second provides information under 25 mm radial ice load. Subsequently, the dynamic analysis is carried out with a death element option to simulate the break in the conductor under ice loading.

3.6.4 Static Analysis to Estimate Residual Static Load

To estimate the static residual load under a steady state condition, two approaches are used. In the first approach, the dynamic analysis is carried out with increased material damping properties to ensure that a steady state condition is reached quickly. The objective here is not to estimate the peak dynamic load rather the steady state residual load and therefore the increased damping properties will only help to obtain the static equilibrium within a short time period.

In the second approach, a static analysis is carried out by simulating the conductor rupture with a static load approximately equal to the conductor tension applied at the bottom node of the insulator where the conductor was attached (See Figure 3.8). This is necessary to avoid numerical instability in the analysis due to the pin connectivity of the insulator to the tower

The load equivalent to the conductor tension is applied in the opposite direction of the swing of the insulator. Using a load function that drops gradually from full tension to zero value, the static analysis is performed (See Figure 3.9). This procedure gives the final static equilibrium configuration of the line system after the conductor break is simulated. It was found in this study that the both methods give identical results with respect to static residual forces.

Figure 3.8 Insulator swinging direction after the conductor rupture

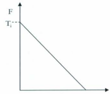

Figure 3.9 Variation of Load for Residual Analysis

3.7 Broken Conductor Analysis (EPRI Wisconsin tests).

Conductor rupture in the span next to the left anchor in Figure 3.1 (span 2 Test No. IIIR1 to IIIL3) was simulated by invoking the death element option in ADINA. The transient and steady state analyses were carried out to obtain the peak dynamic and residual forces in the insulators and members of the tower T3. The predicted time histories of insulator tension at tower T3 for the tests IIIR1 and

IIIL1, IIL2 and IIIL3 are presented in Figures 3.10 to 3.14 respectively. These figures also compare the numerical results with those data obtained from the full scale tests. From these figures, it can be seen that the numerical results obtained from this study compare well with those obtained from the full scale tests.

Table 3.4 presents the comparison of conductor tensions (peak and residual) as well as the leg member forces from tower T3 with those obtained from the full scale tests. It is understood from Ref [5] that prior to the conductor rupture, the strain gauges at all tower members were initialized and therefore, the peak forces reported do not include the effects of the initial compressive forces in the members due to dead loads.. However in the ADINA model, the dead load effect is automatically included in the final output results. Accordingly, the initial member forces due to self-weight were subtracted from the maximum peak forces to compare the values with the full scale test results. From the table 3.4, it can be seen that the results obtained from the numerical model compare well in most cases with those obtained from the full scale tests.

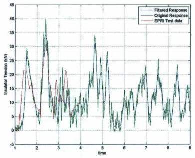

Figure 3.10 Insulator Tension Time History for the Test Case IIIR1

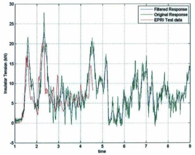

Figure 3.11 Insulator Tension Time History for the Test Case IIIL1

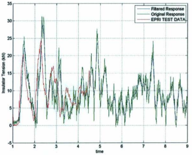

Figure 3.12 Insulator Tension Time History for the Test Case IIIL2

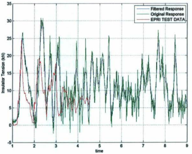

Figure 3.13 Insulator Tension Time History for the Test Case IIIL3

Table 3.4 Broken conductor tests – Force exerted on Tower T3 Comparison

	Initial	Finl			
Test Number	Initial Conductor Tension (N)	Residual Conductor tension (N) as reported in Ref {5 and 8]	Residual Conductor tension (N) (Present study)	Peak Forces (N) as reported in Ref (5 and 8)	Peak Forces (N) (Present study)
III.R.1	18639	10987	11054	31883	39440
III.R.2	19130	10987	11151	34727	35437
III.R.3	-	-	12257	-	43300
III.L.1	12459	7063	7112	20307	23429
III.L.2	17756	8731	8520	24623	31265
III.L.3	21288	9320	9323	24623	33702
IIIR1Leg1	-	-	-	34826	48095
IIIR1Leg2	-	-	-	40123	44743
IIIR1Leg3	-	-	-	40888	44365
IIIR1Leg4	-	-	-	52248	48552
IIIR2Leg1	-	-	-	38612	58502
IIIR2Leg2	-	-	-	51493	53226
IIIR2Leg3	-	-	-	53003	52512
IIIR2Leg4	-	-	-	58301	59251
IIIL1Leg1	-	-	-	16657	26596
IIIL1Leg2	-	-	-	28017	32566
IIIL1Leg3	-	-	-	27262	32465
IIIL1Leg4	-	-	-	25741	26852
IIIL2Leg1	-	-	-	35581	43291
IIIL2leg2	-	-	-	36336	55140
IIIL2leg3	-	-	-	33315	48624
IIIL2leg4	-	-	-	44675	48722
IIIL3Leg1	-	-	-	62843	66902
IIIL3leg2	-	-	-	74203	68141
IIIL3leg3	-	-	-	65109	71596
IIIL3leg4	-	-	-	74958	63226

3.8 Conclusion

This chapter presented the numerical model developed for the Wisconsin test transmission line. The numerical analysis provided time histories of conductor and insulator tension, member forces in the tower, nodal displacements etc. It can be concluded from the results that a reasonable comparison was obtained with those obtained during the tests.

4.0 MODELING

The main objective of this section is to present the various structural models and the properties that were used in developing the line models.

4.1 Structure Modeling

In order to determine the peak dynamic and the static residual longitudinal forces that act on the structure due to sudden conductor rupture, the transmission line models were developed using four different structure types. The following structure types are considered in modeling the transmission lines;

1) Self-supported steel lattice tower for which the design drawings were acquired from Manitoba Hydro.
2) Guyed-V steel lattice tower for which the design drawings were acquired from Newfoundland & Labrador Hydro (NLH), Nalcor Energy
3) H-frame wood pole structure – Type A, suspension structure-design was done by NLH, Nalcor Energy
4) Steel tubular pole structure - design details obtained from Bonneville Power Administration (BPA)

4.1.1 Self-supported Steel Lattice Tower

The self-supported steel lattice tower drawings were supplied by Manitoba Hydro for a single circuit 230 kV structure. The tower was designed for a span of 214m to provide the adequate ground clearance under one inch radial ice load. The self-supported steel lattice tower was broken into five components that made up the basic tower configuration. Two sets of leg extension (3048 mm and 9144 mm) are available to develop different tower heights as required by the user. The limit span for these extensions is 428m under one inch radial ice.

The main structural components are: lower tower body, upper tower body, support arm and cross arm as shown in Figure 4.1. Each tower component was first modeled in AutoCAD using a local coordinate system. The origin was always taken as the centerline of the lower most plane. Modeling each component in AutoCAD made it possible to extract the information on nodal co-ordinates, elements connectivity and the members' section properties. A program was written in java script which appended the above information to generate the finite element data in a format that can be used in ADINA directly. Sections 4.2 and 4.3 present the finite element models for different components. The basic tower as assembled, the tower with 3048mm leg extension and the tower with 9144mm leg extensions are also shown in Figure 4.4.

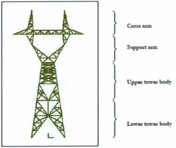

Figure 4.1 Basic tower components

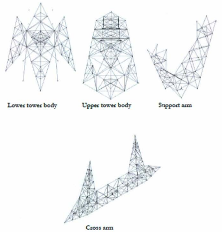

Figure 4.2 Various components of self-supported steel lattice tower

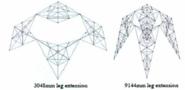

Figure 4.3 Self-supported steel lattice tower's leg extensions

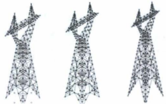

Figure 4.4 Fully configured self-supported steel lattice tower

4.1.2 Guyed-V Steel Lattice Tower

The Guyed-V steel lattice tower design drawings were provided by Newfoundland and Labrador Hydro (NLH) for a 230kV suspension structure. The tower was designed for a span of 428m. to provide the adequate ground clearance under a 25mm radial ice load. The tower considered for this analysis consists of the basic tower body with two mast extensions (see Figure 4.6).

The basic Guyed-V steel lattice tower is broken into three main components; cross arm, upper mast, and bottom mast as shown in Figure 4.5. To increase the tower height, the mast extensions can be used. These mast extensions can be added in various combinations between the upper and lower mast sections to obtain the required tower height. The maximum height can be up to 27.5m (90 feet) (a maximum mast extension of 12.19m (40 feet). The limit span for these extensions is 428 m under 25 mm radial ice

The Guyed-V steel lattice tower modeling was done following the methodology used in the case of self-supported steel lattice tower (refer to previous section for modeling). The modeling of the mast components (lower mast, upper mast and the mast extensions in Figure 4.6 were done by generating the mast geometric model in AUTOCAD. The nodal coordinates, element connectivity and type of members were extracted from AUTOCAD file for the assembly of these components. After assembling the lower mast, mast extensions and the upper mast, the nodal co-ordinates of all the joints were transformed into global coordinate system. Taking advantage of the symmetry of the assembled mast with one symmetric section of the cross arm about the longitudinal plane, the other symmetric portion of the tower is modeled. Later, guy wires were modeled appropriately and the fully assembled tower is shown in Figure 4.7.

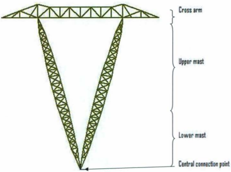

Figure 4.5 Basic guyed-V steel lattice tower

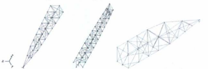

Lower mast Top mast Symmetric section of cross arm

6.1 m Mast extension

4.6 m Mast extension

Figure 4.6 Various components of the guyed-V steel lattice tower

Figure 4.7 Fully configured guyed-V steel lattice towers

4.1.3 Pseudo-elements

Self supported steel lattice tower and guyed-V steel lattice towers were modeled using three dimensional truss elements. In these towers, the outside leg members are often continuous and are braced at each panel level. These members resist some bending moments and ideally should be modeled with beam elements. However, the modeling of these members using truss elements will not cause a significant inaccuracy in the member forces. This was validated earlier for the Wisconsin test line. However, at certain panel (diaphragm at the horizontal plane) location, the truss element members may not be connected in all three directions at a node point (two along the horizontal plane and one along the vertical direction. This will create numerical instability because the assembled stiffness matrix may not be positive definite (positive determinant) and therefore some correction is necessary in the modeling. To achieve the numerical stability, a pseudo-element or dummy element having cross sectional area of 1 mm^2 was placed in order to form a truss that will make the model numerically stable.

4.1.4 H-frame Wood Pole Structure

A special H-frame wood pole structure was designed for a limit span of 428m to support 25mm (one inch) radial ice load. However, the structure height was not adequate to provide sufficient ground clearance under the ice load. Therefore, the span was limited to 214m to provide the adequate ground clearance under 25mm (one inch) ice load. The details of the design were provided by Newfoundland and Labrador Hydro. The schematic of the H-frame wood pole structure is given in Figure 4.8. The pole diameter at the base is 0.44 meter and 0.24 meter at the top with a linear taper of 0.0099 m/m The structural data for other components are given in the Table 4.1

Table 4.1 Structural Data for the components of H-frame wood pole structure

Cross arm	Cross brace	Knee brace
Length = 13.71 m	-	-
Depth = 0.1524 m	Depth = 0.1397 m	Depth = 0.12 m
Width = 0.26 m	Width = 0.1397 m	Width = 0.078 m
E = 13237.91 MPa	E = 12410.5 MPa	E = 13237.9 MPa
Weight= 4560.168 N	Weight = 110.93 N/m	Weight = 88.783 N/m

H-frame wood pole structure in Figure 4.8 was modeled using three dimensional beam elements. Each pole is divided into fifteen (15) beam elements. Since the cross section is varying across the height of the pole structure, the average diameter based on the diameters at the ends of each element is used to model the cross sectional area of the beam element.

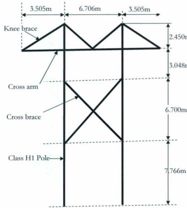

Figure 4.8 H-frame wood pole structure

4.1.5 Steel Tubular Pole Structure

The steel tubular pole structure drawings were supplied by BPA. The schematic of the steel tubular pole structure is given in Figure 4.9. The typical pole height is 30.48m (100 foot). The pole structure was suitable for a limit span of 214 m to support 25mm (one inch) radial ice load and to provide adequate ground clearance. The cross section is a regular twelve face polygonal type. At the base, the dimension across the flats is 0.80m (31.38inches and the plate thickness is 7.14mm (0.28 inches). The pole has a taper of 0.016 m/m (0.19 in/ft.) The plate thickness is 7.14mm that is constant from the base to a height of 19.8m (65 foot). The remaining of the pole section has a plate thickness of 4.76 mm (0.19 inches). The three arms of length 3.31 m are inclined upward with a 3^{o} angle from the horizontal. The arm cross section is hollow irregular hexagon (elliptical) (see figure 4.10) with a plate thickness of 6.35 mm. Steel tubular pole structure was also modeled using the methodology as outlined in Section 4.1.4. Each pole is divided into a number of beam elements. Since the cross section is polygonal, the element section properties (area, moment of inertia, torsional constant) were calculated using the average pole dimensions between the two consecutive nodes. The cross arm was also modeled as beam elements taking into account the irregular shape. Three beam elements were used to model the cross arm with appropriate section properties.

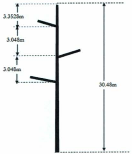

Figure 4.9 Steel tubular pole structure

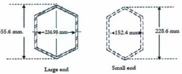

Figure 4.10 Cross section details of the arm

4.2 Transmission Line Modeling

The three distinct terrain types with 31 spans were considered as follows (data provided by NLH, Nalcor Energy)

1. Flat terrain
2. Hilly terrain
3. Valley terrain

The conductors strung between the towers were modeled using three dimensional truss elements with initial strain corresponding to the initial conductor tension. The nodal co-ordinates in the conductor model are generated using the coordinates of end points of the conductor in each of the span. Since the conductor and guy wires were modeled as assembly of tension only truss elements a multi-linear material model was used i.e. the modulus of elasticity is zero if the axial strain is compressive and modulus of elasticity is prescribed only when axial strain is positive. A java script was written to generate the input file data automatically in a format required for ADINA software.

The following input data was required to generate the data for transmission line model:

i) Conductor prosperities – area of cross section, weight density per unit length, modulus of elasticity and initial conductor tension.

ii) The foundation co-ordinates of each the tower location with respect to the first tower i.e. x co-ordinate along the transverse direction of the line, y co-ordinate along the longitudinal direction of the line, and z co-ordinate, describing the tower foundation elevation, conductor attachment point with insulator co-ordinates with respect to the origin of the tower co-ordinate system and the insulator string length.

iii) Data file that contains nodal point coordinates, line/element connectivity information, element cross sectional properties, weight density and modulus of elasticity.

The transmission lines were modeled using 31 tower structures. For the hilly terrain, the 16^{th} structure was placed on the top of the hill while structure no 1 and 31 are located at the ends of the line respectively. The same slope was used to model the hilly and the valley terrains. The slope was 18 m increase in height over each span length of 428.42m or a 9 m increase in height over each span length of 214.21. This was the converse for the valley terrain. A section of the model for each of the terrains are shown in Figures 4.11 to 4.13

Table 4.2. Configuration for transmission line models for any terrain

Tower type	Basic self supported steel lattice tower		Self supported steel lattice tower with 3048 mm leg extension		Self supported steel lattice tower with 9144 mm leg extension		H-frame wood pole structure		Steel tubular pole structure		Guyed-V steel lattice tower	
Insulator String Length (m)	214.21		428.42		428.42		428.42		214.21		428.42	
Insulator String Length (m)	2.12	3.1	2.12	3.1	2.12	3.1	2.12	3.1	2.12	3.1	2.12	3.1
Initial tension (% of RTS)	15%; 20%; 25%		15%; 20%; 25%		15%; 20%; 25%		15%; 20%; 25%		15%; 20%; 25%		15%; 20%; 25%	

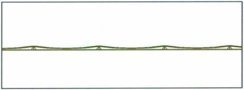

Figure 4.11 Level terrain

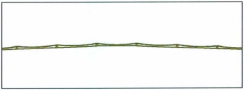

Figure 4.12 Hilly terrain

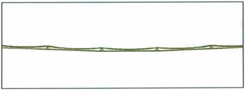

Figure 4.13 Valley terrain

Figures 4.14 to 4.17 present the line models in ADINA with self-supported steel lattice tower, guyed-V steel lattice tower, the steel tubular pole structure and H-frame wood pole structure respectively.

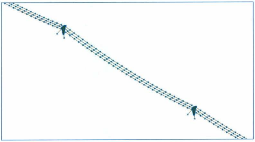

Figure 4.14 Section of the line with guyed-V steel lattice tower

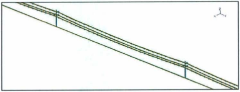

Figure 4.15 Section of the line with steel tubular pole structure

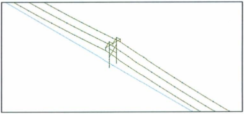

Figure 4.16 Section of the line with H-frame wood pole structure

5.0 FREE VIBRATION ANALYSIS AND DAMPING

The first step in a transient dynamic analysis using either implicit or explicit integration procedure is to estimate the appropriate damping parameters. In the transient analysis of a transmission line due to conductor rupture, one needs to use different damping values for the conductor (a flexible system) and the tower (a less flexible system). Rayleigh damping is used, and ADINA software can prescribe damping values for different element groups. In this chapter free vibration analysis is presented to provide longitudinal frequencies for the structure and the in-plane frequencies of the line section.

5.1 Free Vibration Analysis of Towers

For conducting free vibration analysis, a lumped mass model was used. The longitudinal bending modes of the supporting structures are important for the transient analysis transmission line. By examining the mode shapes of the supporting structures, these longitudinal bending modes were identified. The longitudinal mode shapes for various structure types are shown in Figures 5.1 to 5.6. In general, the first longitudinal bending mode shape may not be associated with the first natural frequency in all cases. The natural frequencies for all supporting structures are given in Tables 5.1 to 5.6. The longitudinal bending frequencies are shown in red in these tables.

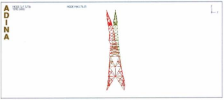

Figure 5.1Longitudinal bending mode of basic self-supported steel lattice tower

Table 5.1 Natural frequencies for basic self-supported steel lattice tower

Frequency (rads/Sec)	Frequency (Hz)	Period (Seconds)	Mode Shape
22.19	3.531	0.2832	1
23.47 *	3.736	0.2677	2
44.1	7.018	0.1425	3

- longitudinal bending mode

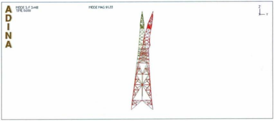

Figure 5.2 Longitudinal bending mode for self-supported steel lattice tower with 3048 mm leg extension

Table 5.2 Natural frequencies for self-supported steel lattice tower with 3048 mm leg extension

Frequency (rads/Sec)	Frequency (Hz)	Period (Seconds)	Mode Shape
20.67	3.29	0.304	1
21.67*	3.448	0.29	2
43.68	6.952	0.1439	3

* longitudinal bending mode

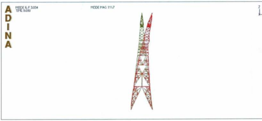

Figure 5.3 Longitudinal bending mode for self-supported steel lattice tower with 9144 mm leg extension

Table 5.3 Natural frequencies for self-supported lattice tower with 9144 mm leg extension

Frequency (rads/s)	Frequency (Hz)	Period (seconds)	Mode
18.4	2.929	0.3414	1
19.07*	3.034	0.3296	2
40.18	6.395	0.1564	3

- * longitudinal bending mode

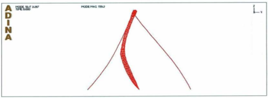

Figure 5.4 Longitudinal bending mode for guyed V steel lattice tower with 10.67 m (35 Foot Extension)

Table 5.4 Natural frequencies for guyed V steel lattice tower with 10.67 m (35 Foot Extension)

Frequency (rads/s)	Frequency (Hz)	Period (seconds)	Mode
1.29E+01	2.06E+00	4.86E-01	1
1.43E+01	2.27E+00	4.41E-01	2
3.20E+01	5.09E+00	1.96E-01	3

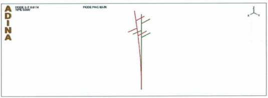

Figure 5.5 Longitudinal bending mode for steel tubular pole structure

Table 5.5 Natural frequencies for steel tubular pole structure

Frequency (rads/s)	Frequency (Hz)	Period (seconds)	Mode
5.71E+00	9.09E-01	1.10E+00	1
5.73E+00	9.11E-01	1.10E+00	2
5.25E+01	8.35E+00	1.20E-01	3

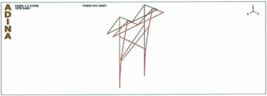

Figure 5.6 Longitudinal bending mode for H-frame wood pole structure

Table 5.6 Natural frequencies for H-frame wood pole structure

Frequency (rads/s)	Frequency (Hz)	Period (seconds)	Mode
3.37E+00	5.36E-01	1.87E+00	1
6.91E+00	1.10E+00	9.09E-01	2
1.22E+01	1.95E+00	5.14E-01	3

5.2 Free Vibration Analysis of Transmission Line

The frequency analyses were carried out for a section of transmission line modeled with the input data given in Table 5.7. The relevant frequencies and the mode shapes were identified for further dynamic analyses. The frequency values for the three initial tensions considered are given in Table 5.8

In the analysis, it was noted that the natural frequency of the line depends only on the initial conductor tension and span length. The frequency was not dependent on other line parameters such as structure type, insulator length and the terrain type.

Table 5.7. Input data for transmission line models for a given terrain

Terrain										
Tower Type	Basic self-supported steel lattice tower		Self-supported steel lattice tower with 3048 leg extension		Self-supported steel lattice tower with 9144 mm leg extension		H-frame wood pole structure		Steel tubular pole structure	
Span (m)	214.21		428.42		428.42		214.21		214.21	
Insulator String Length (m)	2.12	3.1	2.12	3.1	2.12	3.1	2.12	3.1	2.12	3.1
Initial tension (% of RTS)	15; 20; 25		15; 20; 25		15; 20; 25		15; 20; 25		15; 20; 25	

Table 5.8 Transmission line frequencies

Spans length	Initial tension (% RTS)	Frequency ω (rads/s)
428.42 m	15	0.26
	20	0.38
	25	0.49
214.21 m	15	0.88
	20	1.17
	25	1.41

5.3 Damping Matrix

For a transient dynamic analysis, the damping matrix [C] is required. To construct the damping matrix, Rayleigh damping coefficients are used in conjunction with the mass and stiffness matrices. The damping matrix is given by

$$[C] = \alpha\,[M] + \beta\,[K] \tag{5.1}$$

Where α and β are Rayleigh damping coefficients, [M] and [K] are total system mass and stiffness matrices.

The critical damping ratio ω_i for mode, i, is given in terms of Raleigh damping coefficients as

$$\xi_i = \frac{\alpha}{2\omega_i} + \frac{\beta\omega_i}{2} \tag{5.2}$$

Where ω_i, is natural frequency of the system in i^{th} mode of vibration

In the present analysis, a damping matrix proportional to mass matrix is used which means that β is equal to zero. As a result we can calculate α as follows. The matrix has only diagonal elements.

$$\alpha = 2\xi\omega_i \tag{5.3}$$

A damping ratio $\xi = 0.02$ for conductor and a damping ratio $\xi = 0.1$ for tower were used with the natural frequencies of these two element groups to construct the damping matrix. Rayleigh damping coefficients for all tower types are given in Table 5.9 and for conductors are given in Table 5.10.

Table 5.9 Rayleigh damping constant α for supporting structures

Structure Type	Frequency, ω (Rads/s) YZ Mode	Rayleigh Constant α ($\xi = 0.1$)
Self-supported steel lattice tower	23.47	4.69
Self-supported steel lattice tower with 3048mm leg extension	21.67	4.33
Self-supported steel lattice tower with 9144mm leg extension	19.09	3.82
Guyed V steel lattice tower	14.25	2.85
Steel tubular pole structure	5.727	1.15
H-frame wood pole structure	3.367	0.67

Table 5.10 - Summary of conductor damping coefficients

Spans length	Initial tension (% RTS)	Freqency, ω (rads/s)	Rayleigh Constant α ($\xi = 0.02$)
428.42 m	15	0.26	0.0104
	20	0.38	0.0151
	25	0.49	0.0195
214.21 m	15	0.88	0.0353
	20	1.17	0.0469
	25	1.41	0.0565

6.0 STATIC AND DYNAMIC ANALYSIS

Using the procedure as outlined in Section 3.6, static and dynamic analyses were carried out for 230kV overhead lines modeled with four types of structures. These structure types are: (1) Self-supported steel lattice tower (2) Guyed-V steel lattice tower (3) Steel tubular pole structure and (4) H-frame wood pole structure. The primary objective is to study the effect of structural flexibility on the dynamic peak and static residual conductor tensions in the span next to the break. The details of the analyses are presented in this chapter.

6.1 The Effect of Structural Flexibility on Residual Conductor Tension

EPRI study [13] has shown that after a conductor rupture, the magnitude of the static residual force on a structure away from the failure zone can be estimated based on the initial conductor tension, longitudinal load factor for the structure, correction factors for span/insulator ratio and the structural flexibility. Longitudinal Load Factor (LLF) is defined as a function of the response coefficient and span/sag ratio. The response coefficient is determined from test results. The Span/Insulator correction Factor ($CF_{S/I}$) is defined as ($CF_{S/I}$) = (1-((S/I)/N)), where N is the span number, S is span length and I is the insulator length. There are a number of other formulae used for the design and prediction of cascade failures in tower design.

The flexibility correction factor is defined as the ratio of the residual conductor tension for a flexible structure (e.g. N^{th} structure) to the residual tension for a rigid structure. In the EPRI report, this flexibility correction factor for N^{th} structure is computed based on an empirical formula and given as

$$C = e^{-\left(\frac{(1/k_n)}{200}\right)} \tag{6.1}$$

where

C = Structural flexibility correction factor for N^{th} structure

$1/k_n$ = Structural flexibility of N^{th} structure in m/kN

The structure's stiffness was obtained by applying a unit load at the center of the cross arm. Table 6.1 presents the data for all four structure types.

Table 6.1 Stiffness and flexibility values for support structures

Structure type	Stiffness (kN/m)	Span (m)
Self supported Lattice Tower(basic tower)	785.90	214.12
Lattice self supported tower with 3048 mm leg extensions	685.89	428.42
Lattice self supported tower with 9144 mm leg extensions	548.35	428.42
Guyed-V tower	251.68	428.42
Steel Pole structure	28.54	214.21
Wood pole H-Frame structure	17.03	214.21

Figure 6.1 presents the correction factor plot for a wide range of structural flexibility values given in Ref.[13]. The figure was modified to accommodate the flexibility value up to 0.15 m/kN. A reference correction factor of 1.0 is used for a rigid structure and a factor of 0.7 refers to a very flexible structure.

The EPRI study suggested that for a self-supported heavy angle tower or a dead end steel tower, the values could range from 5.7 to 34.24E-03 (m/kN). For a self-supported lattice tangent tower, typical flexibility value can range between 34.3E-03 to 68.5E-03 (m/kN) while for a H-frame wood pole or a steel pole structure; this value could range from 68E-03 to (m/kN) 342 E-03 respectively. Table 6.2 presents the flexibility data for the structures used in this study and compares these values with those suggested in the EPRI study [13]. It appears that both the Guyed-V and self-supported steel lattice towers are considerably stiffer (almost rigid) compared to the values suggested in the EPRI report. This is mainly due to the difference in tower design. The flexibility properties for the steel tubular pole structure and the H-frame wood pole structure are reasonable when compared to the values suggested in reference [13].

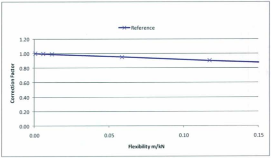

Figure 6.1 Correction factor versus structural flexibility values (Ref [13], modified)

Table 6.2 Comparison of flexibility values -between the structures used in this study and the values suggested in the EPRI report

Structure Types	Flexibility Value given in Reference [13] (10^{-3}m/KN)		Flexibility value used in this study (10^{-3}m/kN)
	Upper Value	Lower Value	
Tangent (Self supported) or Guyed-V	68	34	1.27 to 3.9
Tangent steel pole or wood pole structures	342	68	35 to 58

In this section, a transmission line modeled with H-frame wood pole structures is used to study the effect of structural flexibility on the residual conductor tension. In the analysis, the following two cases are considered:

(i) CASE A - large displacement analysis for both conductor and structure (flexible).

(ii) CASE B - large displacement analysis for the conductor and small displacement analysis for the structure (stiff).

To simulate the variations in structural flexibility, Young's moduli of the structural wood members (poles, cross-arms etc.) were changed. The line model used a span of 214.21 m with an initial conductor tension of 20% RTS (Rated Tensile Strength). A line model with a span of 428.42m was also used to study the span effect on the flexibility correction factor. The conductor rupture was simulated for the span next to the structure number 16. The numerical results for the above two cases studied are given in Table 6-3 and are compared with the values given in the EPRI study [13] Figure 6-2 presents the comparison plots.

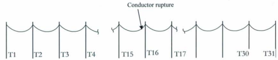

Figure 6.2 Line configuration showing the location of conductor rupture

The correction factors for the two cases are presented by the following empirical equations.

For CASE A $C = e^{-0.003/k}$

$$(6.2)$$

For CASE B $C = e^{-0.002/k}$

$$(6.3)$$

For CASE A with 428m span, $C = e^{-0.001/k}$

$$(6.4)$$

Table 6.3 Flexibility correction factors

Initial conductor tension 20% RTS							
	Large displacement analysis - Case A (Span 214.21 m)		Large displacement analysis - Case A (Span 428.42 m)		Small displacement analysis - Case B (Span 214.21 m)		Reference correction factor
Flexibility (m/kN)	Residual load (kN)	Correction factor	Residual load (kN)	Correction factor	Residual load (kN)	Correction factor	EXP(-(1/k))
0	12.67	1.00	20.18	1.00	12.67	1.00	1.00
0.01	12.06	0.95	19.54	0.97	12.07	0.95	0.99
0.01	11.51	0.91	18.92	0.94	11.54	0.91	0.99
0.06	9.15	0.72	15.92	0.79	9.55	0.75	0.95
0.12	7.83	0.62	14.20	0.70	8.77	0.69	0.90
0.18	7.09	0.56	13.44	0.67	8.38	0.66	0.86

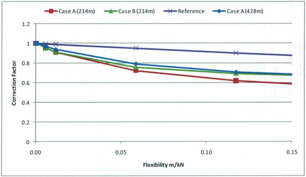

Figure 6.3 Flexibility correction factors (modified after [13])

6.2 The Effect of Structural Flexibility on Dynamic Peak Conductor Tension

Dynamic simulation analyses were carried out on two groups of transmission lines. Each group consists of three separate lines. Each line has one specific structure type. These structure types are: (1) Self-supported steel lattice tower with 3048mm leg extensions (2) Self-supported steel lattice tower with 9114mm leg extensions and (3) Guyed-V steel lattice tower. The first group has a typical span of 428m and have the same span/sag and the span/insulator ratios.

The second group also consists of three structure types; (1) Self-supported steel lattice tower (basic tower height), (2) Steel tubular pole structure and (3) H-frame wood pole structure. All these lines have also equal spans of 214m and the same span/ sag and the span/insulator ratios.

6.2.1 Simulation Results for Group 1

Figure 6.4 presents a typical time history plot for the conductor tension in a line modeled with self-supported steel lattice tower. From the figure it can be seen that the maximum peak dynamic force is 50.03 kN

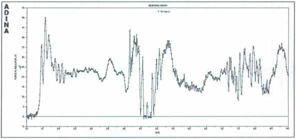

Figure 6.4 Time history of conductor tension (Self-supported steel lattice tower with 3048mm leg extensions)

Figure 6.5 presents a typical time history plot for the conductor tension in a line modeled with self-supported steel lattice tower with 9114mm leg extensions. From the figure it can be seen that the maximum dynamic peak force is 49.13 kN.

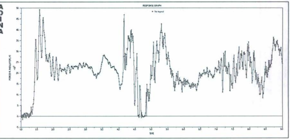

Figure 6.5 Time history of conductor tension (Self-supported steel lattice tower with 9144 mm leg extensions)

Figure 6.6 presents a typical time history plot for the conductor tension in a line modeled with Guyed-V steel lattice tower. From the figure it can be seen that the maximum peak force is 46.87 kN.

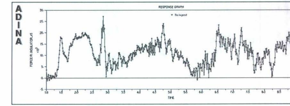

Figure 6.6 Time history of conductor tension (Guyed-V steel lattice tower)

6.2.2 Simulation Results for Group 2

Figure 6.7 presents a typical time history plot for the conductor tension in a line modeled with self-supported steel lattice tower (basic tower type).From the figure it can be seen that the maximum peak force is 39.44 kN

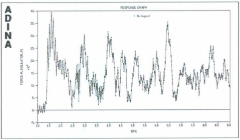

Figure 6.7 Time history of conductor tension (Basic self-supported steel lattice tower)

Figure 6.8 presents a typical time history plot for the conductor tension in a line modeled with steel tubular pole structure. From the figure it can be seen that the maximum peak force is 27.14 kN

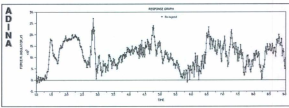

Figure 6.8 Time history of conductor tension (Steel tubular pole structure)

Figure 6.9 presents a typical time history plot for the conductor tension in a line modeled with the H-frame wood pole structure. From the figure it can be seen that the maximum peak force is 44.0 kN.

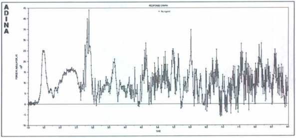

Figure 6.9 Time history of conductor tension (H-frame wood pole structure)

Table 6.4 Peak and residual conductor tensions for Group 1 (span/sag =32)

Group 1			
Structure type	Stiffness (kN/m)	Maximum peak force (kN)	Residual load (kN)
Lattice self-supported tower with 3048 mm leg extension	685.89	50.03	20.17
Lattice self-supported tower with 9144 mm leg extension	548.35	49.17	20.10
Guyed-V tower	251.68	46.87	19.84

Table 6.5 Peak and residual conductor tensions for Group 2 (span/sag =65)

Group 2			
Structure type	Stiffness (kN/m)	Maximum peak force (kN)	Residual load (kN)
Lattice self-supported basic tower	785.9	39.44	12.60
Steel tubular pole structure	28.517	27.15	10.26
H-frame wooden pole structure	17.028	44.00	9.14

i) From the examination of the above results, it is observed that for lines modeled under group 1 with two types of self-supported structures, the maximum peak dynamic conductor tension is invariant to the selected stiffness values. (Figures 6.4, 6.5). However for the guyed-V steel lattice tower, there is a 10% reduction in the peak force because the guyed-V steel lattice tower has a considerable lower stiffness value compared to the other two structure types

ii) For lines modeled under group 2, it is seen that the steel tubular pole structure is subjected to a reduced dynamic peak load when compared to the basic rigid structure type. However for some unknown reasons, this was not observed for the H-frame wooden pole structure although both these structures are flexible structures (Refer to Table 6.1). For these two types of flexible structures, it is believed that the structure's layout and mass have an impact on the peak dynamic force in addition to the structural flexibility values and therefore, a separate study was carried out to understand this issue

iii) The computed residual loads on all structure types are affected by the flexibility values. This is in line with the EPRI study results and the other past studies.

6.2.3 The Effect of the H-frame Cross Arm Mass on Dynamic Peak Conductor Tension

In order to study the effect of the cross arm mass on the peak dynamic tension, a line modeled with the H-frame wooden pole structure is considered. The dynamic analysis was conducted for two specifics cases: (1) the original mass of the cross arm and (2) the reduced mass for the cross arm. The reduction of the cross arm mass was achieved by changing the density value while keeping the same stiffness property. The dynamic peak conductor tensions obtained in both cases are shown in Table 6.6.

Table 6.6 The Effect of cross arm mass on peak conductor tension

		Wood pole with original cross arm mass Peak dynamic conductor tension (kN)			Wood pole with reduced cross arm mass Peak dynamic conductor tension (kN)		
Insulator Length	RTS	Left Phase	Middle Phase	Right Phase	Left Phase	Middle Phase	Right Phase
2-12 m	15.00	24.07	26.84	24.07	16.49	23.20	16.49
	20.00	26.52	44.88	26.53	18.54	31.24	18.23
	25.00	34.11	53.83	34.11	20.19	36.88	20.19
3.1 m	15.00	21.19	27.36	21.95	17.39	23.95	20.19
	20.00	20.75	36.70	20.75	16.33	24.16	16.32
	25.00	30.70	47.92	29.45	24.01	37.78	24.01

It can be seen from the table that the reduction in the structural mass has a considerable impact on the peak dynamic conductor tension (hence the force on the insulator). The structural mass of the cross arm of the H-frame wood pole structure is 2.5 times that of the tubular pole cross arm. The results in Table 6.6 show the effects of the mass on the dynamic peak force. In this study all structures are framed except the pole structure. Therefore, the shape of the structure may also influence the dynamic behaviour and hence, the peak force predicted. More investigation is needed to understand the issue.

6.3 Impact Factors

Dynamic simulations studies were carried out using the line parameters as presented in Table 6.7. For each case, two insulator string lengths (2.12 m and 3.1 m) were used.

The impact factors as proposed by Govers [4], the ratio of maximum transient longitudinal force to the initial conductor tension (IFI), and the ratio of maximum transient longitudinal force to the residual conductor tension (IFF) are used to present the dynamic simulation results. The residual ratio (RR) defined as the ratio of residual force to the initial conductor tension was also used to present the steady state simulation results.

From the simulation results, these factors were calculated and presented against the non-dimensional parameters as defined below

k′ = Tower Stiffness/weight of the conductor per unit length

Span sag ratio= Length of span/sag

Supporting structure's stiffness's and sags corresponding to the initial conductor tension are given in the Table 6.7. All these calculations are done for two span/insulator ratios.

Figures 6.10 and 6.11 show the variation of residual ratio (RR) for transmission line models with span/sag ratio for different tower types. From these figures it is inferred that residual ratio decreases with increasing span/sag ratio. The residual ratio is also higher for stiff structures when compared to more flexible structures. Residual ratio increases with increase in span/insulator length.

Figures 6.12 and 6.13 show the variation of impact factor (IFF) for transmission line models with span/sag ratio for different tower types. From these figures it is inferred that IFF increases with increasing span/sag ratio for more flexible structures. For stiff structures, there is a general trend that IFF decreases with the increase in span/sag ratio. For stiff structures, it does not appear that the span/sag ratio does really affect the IFF values. However the arm impact factor (IFF) increases with the change in the span/insulator ratio.

Table 6.7 Characteristics of transmission line models

<table>
<tr><th rowspan="2">Tower Type</th><th rowspan="2">Stiffness (kN/m)</th><th rowspan="2">Stiffness/conductor weight/unit length</th><th rowspan="2">Span (m)</th><th colspan="3">Sag (m)</th></tr>
<tr><th>15% RTS</th><th>20% RTS</th><th>25% RTS</th></tr>
<tr><td>Wood Pole Structure</td><td>17 028</td><td>1066.25</td><td rowspan="3">214.47</td><td rowspan="3">4.406</td><td rowspan="3">3.304</td><td rowspan="3">2.603</td></tr>
<tr><td>Steel Pole Structure</td><td>28.517</td><td>1785.66</td></tr>
<tr><td>Lattice self supported basic tower</td><td>785.9</td><td>49248.65</td></tr>
<tr><td>V-Guyed Tower</td><td>251.68</td><td>15759.55</td><td rowspan="3">428.93</td><td rowspan="3">17.654</td><td rowspan="3">13.227</td><td rowspan="3">10.577</td></tr>
<tr><td>Lattice self supported basic tower 9144 extension</td><td>548.35</td><td>34336.26</td></tr>
<tr><td>Lattice self supported basic tower 3048 extension</td><td>685.89</td><td>42948.65</td></tr>
</table>

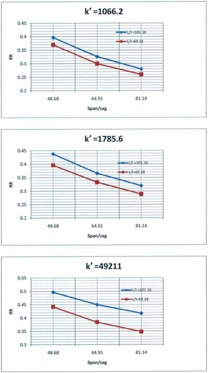

Figure 6.10 Variation of RR with Span/sag (214.47 m)

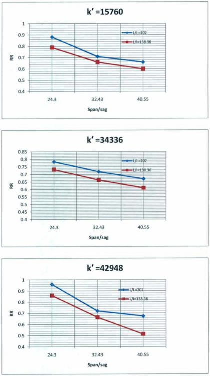

Figure 6.11 Variation of RR with Span/sag (Span 428.95 m)

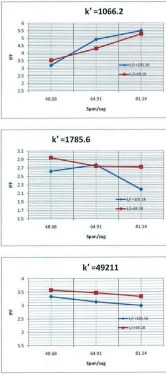

Figure 6.12 Variation of IFF with Span/sag (214.47 m)

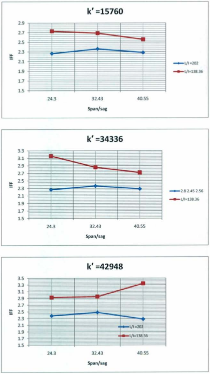

Figure 6.13 Variation of IFF with Span/sag (428.95 m)

6.4 Conclusions

From the foregoing study, it can be inferred that the structural flexibility, span/insulator ratio and the span/sag ratio have considerable effects on the residual conductor tension (hence the insulator force). The peak dynamic tension decreases as the support structure flexibility increases however this is directly affected by the cross arm mass and the shape of the structures used for line modeling. As the cross arm mass is reduced for flexible structures, so does the peak dynamic load. For stiff structures, cross arm mass has very little effect on the peak conductor tension.

For transmission lines modeled with rigid structures, the impact factors are not sensitive to the stiffness values, whereas for lines modeled with flexible structures, (like wood pole and steel tubular pole type structures) the residual ratio (RR) depends on both the stiffness values and span/insulator and span/sag ratios.

7.0 SENSITIVITY ANALYSIS

A sensitivity study was carried out by varying the design parameters that affect the peak and residual conductor tensions. These parameters are initial conductor tensions (15%, 20% and 25% (RTS)), conductor loading (bare conductor, radial ice loads associated with half an inch and one inch ice thicknesses respectively) and three different types of terrain (level, hilly and valley terrains). The simulation test matrix for a typical line model with one particular type of supporting structure is given in Table 7.1. This table provides a number of simulations for each conductor condition; bare conductor, ice loads due to half inch radial and one inch radial ice thicknesses respectively. Therefore, for one structure type, a line model requires 54 simulations to run the sensitivity analysis. For all line models considering the sensitivity of the parameters selected, a total number of 334 simulations are needed.

Table 7.1 Simulation test matrix for a typical line with a particular supporting structure for a particular conductor condition

	Supporting structure type																	
Terrain	Level						Hilly						Valley					
Insulator length	2.12 m			3.1 m			2.12 m			3.1 m			2.12 m			3.1 m		
Initial conductor tension (% of RTS)	15	20	25	15	20	25	15	20	25	15	20	25	15	20	25	15	20	25

From the simulation results, the impact factors IFI (ratio of peak dynamic force to initial conductor tension), IFF (ratio of peak dynamic force to residual tension) and RR (ratio of the residual tension to the initial conductor tension) were calculated and presented in the form of graphs in Figures 7-1 to 7-12 .

The IFI, RR ratios were obtained using the bare conductor initial tension for all conductor conditions i.e. bare conductor, half inch radial ice thickness and one inch radial Ice thickness.

The IFF ratios were calculated using the appropriate residual tension. For example, IFF for one inch radial ice load condition was calculated as the ratio of peak dynamic conductor tension to the residual conductor tension for one inch radial ice load.

Figures 7-1 and 7-3 show the variation of IFI, Figures 7-5 and 7-7 show the variation of IFF and Figures 7-9 and 7-11 show the variation of RR with k' for three different terrain conditions and three initial loading conditions (bare conductor, half an inch and one inch radial ice loads). In all these runs, the transmission line was modeled with 31 spans of equal length of 428m and two types of insulator lengths of 2.12 m and 3.1m (It is a long sentence and putting a lot of information)

Similarly, Figures 7-2 and 7-4 show the variation of IFI, Figures 7-6 to 7-8 show the variation of IFF and Figures 7-10 to 7-12 show the variation of RR with k' for three different terrain conditions and three initial loading for transmission line models with 31 spans of equal span lengths of 214m and insulator lengths of 2.12 m and 3.1m.

Hilly

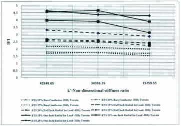

Level

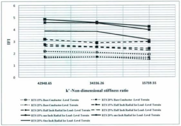

Valley

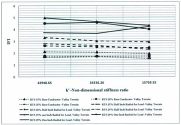

Figure 7.1 Variation IFI vs. k′ (Insulator length 2.12m; Span 428m)

Hilly

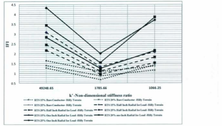

Level

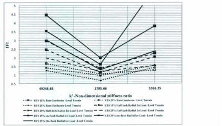

Valley

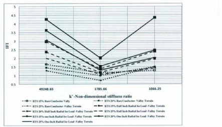

Figure 7.2 Variation IFI vs. k′ (Insulator length 2.12m; Span 214m)

Hilly

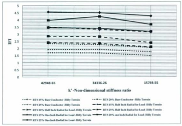

Level

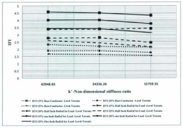

Valley

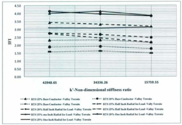

Figure 7.3 Variation IFI vs. k′ (Insulator length 3.1m; Span 428m)

Hilly

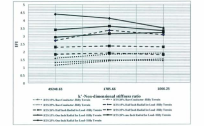

Level

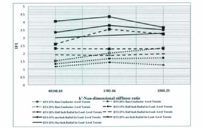

Valley

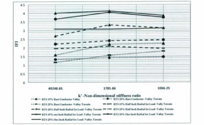

Figure 7.4 Variation IFI vs. k' (Insulator length 3.1m; Span 214m)

Hilly

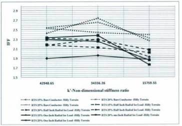

Level

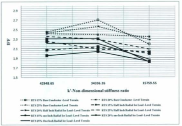

Valley

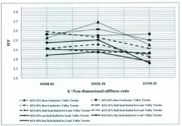

Figure 7.5 Variation IFF vs. k′ (Insulator length 2.12m; Span 428m)

Hilly

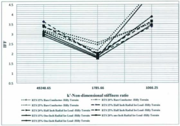

Level

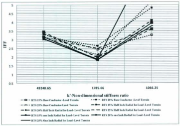

Valley

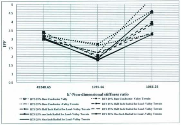

Figure 7.6 Variation IFF vs. k' (Insulator length 2.12m; Span 214m)

Hilly

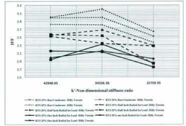

Level

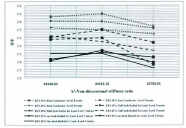

Valley

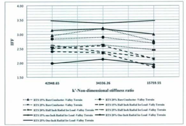

Figure 7.7 Variation IFF vs. k' (Insulator length 3.1m; Span 428m)

Hilly

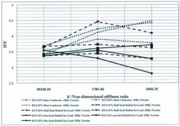

Level

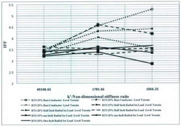

Valley

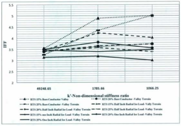

Figure 7.8 Variation IFF vs. k′ (Insulator length 3.1m; Span 214m)

Hilly

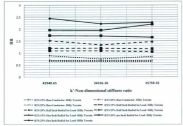

Level

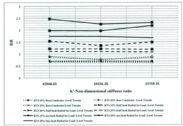

Valley

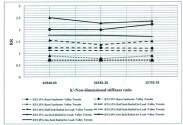

Figure 7.9 Variation RR vs. k′ (Insulator length 2.12m; Span 424m)

Hilly

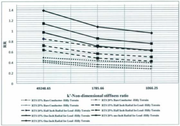

Level

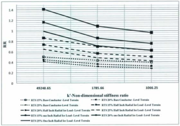

Valley

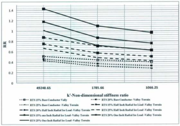

Figure 7.10 Variation RR vs. k'(Insulator length 2.12m; Span 214m)

Hilly

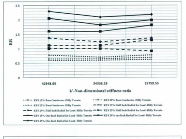

Level

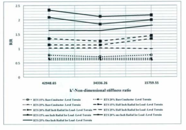

Valley

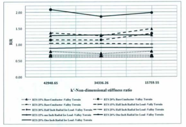

Figure 7.11 Variation RR vs. k′ (Insulator length 3.1m; Span 424m)

Hilly

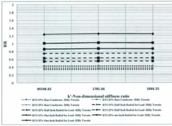

Level

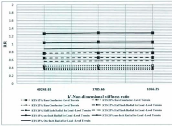

Valley

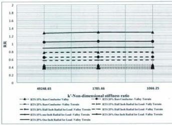

Figure 7.12 Variation RR vs. k′ (Insulator length 3.1m; Span 214m)

From these figures the following points are observed.

a) There is no appreciable effect of insulator string length on the IFI ratios.

b) The impact factor IFI decreases as initial conductor tension is increased.

c) The impact factor IFI is not affected appreciably by the type of tower support used in the transmission line model. The IFI ratios are also not influenced by the terrain type modeled with stiff towers (guyed-V steel lattice tower, self-supported steel lattice towers).

d) The terrain type doesn't significantly influence the impact factors for transmission line models that were considered in this analysis. It should be noted that each transmission line is modeled with one type of terrain and one type of supporting structure. From the parameters used in the sensitivity study, the important design variables that affect the impact factors are initial conductor tension.

Since the impact factors are not affected by terrain type, the average values of impact factors for transmission line that were modeled using different types of supporting structures are presented in the tables 7-2 and 7-3.

From these tables it can seen that for transmission lines modeled using stiff structures, there is no appreciable effect of type of structure on the impact factors.

The impact factors are primarily affected by the initial conductor tension and the type of loading on the conductor (bare versus loaded). As the initial conductor tension increases, the impact factors decreases. The effect of insulator length has more effect on residual ratio than peak impact factors.

For line models that were generated using flexible structures, the structure type and the stiffness have more influence on both peak impact factors and residual ratios.

Table 7.2 Average impact factors for line models with stiff structures (Span Length 428.m)

Insulator length	RTS %	Supporting structure type	k'	Bare conductor			Half inch ice load			one inch ice load		
				IFI	RR	IFF	IFI	RR	IFF	IFI	RR	IFF
2.12m	15	Self-supported steel lattice tower with 3048mm leg extension	42948.6537	2.14	0.89	2.41	3.25	1.53	2.12	2.50	1.11	2.29
		Self-supported steel lattice tower with 9144mm leg extension	34336.2555	2.07	0.76	2.70	2.98	1.35	2.21	2.37	0.96	2.53
		Guyed-V steel lattice tower	15759.55	1.92	0.87	2.21	2.91	1.49	1.95	2.25	1.08	2.12
	20	Self-supported steel lattice tower with 3048mm leg extension	42948.6537	1.74	0.71	2.46	2.65	1.22	2.18	2.05	0.88	2.36
		Self-supported steel lattice tower with 9144mm leg extension	34336.2555	1.70	0.71	2.41	2.52	1.21	2.08	1.98	0.88	2.29
		Guyed-V steel lattice tower	15759.55	1.66	0.70	2.38	2.39	1.19	2.02	1.92	0.86	2.27
	25	Self-supported steel lattice tower with 3048mm leg extension	42948.6537	1.64	0.67	2.46	2.64	1.11	2.39	3.84	1.75	2.20
		Self-supported steel lattice tower with 9144mm leg extension	34336.2555	1.71	0.66	2.58	2.54	1.10	2.31	3.78	1.73	2.18
		Guyed-V steel lattice tower	15759.55	1.50	0.65	2.30	2.23	1.07	2.09	3.48	1.67	1.91
3.1m	15	Self-supported steel lattice tower with 3048mm leg extension	42948.6537	2.32	0.78	2.99	3.43	1.36	2.52	4.67	2.32	2.02
		Self-supported steel lattice tower with 9144mm leg extension	34336.2555	2.26	0.71	3.17	3.34	1.25	2.66	4.49	2.12	2.12
		Guyed-V steel lattice tower	15759.55	2.12	0.78	2.73	3.24	1.43	2.27	4.33	2.18	1.99
	20	Self-supported steel lattice tower with 3048mm leg extension	42948.6537	1.90	0.65	2.91	1.89	0.66	2.89	4.04	2.08	1.95
		Self-supported steel lattice tower with 9144mm leg extension	34336.2555	1.91	0.65	2.93	1.90	0.65	2.91	4.07	1.84	2.21
		Guyed-V steel lattice tower	15759.55	1.76	0.66	2.65	1.76	0.65	2.69	3.75	1.99	1.89
	25	Self-supported steel lattice tower with 3048mm leg extension	42948.6537	1.64	0.61	2.71	2.57	1.02	2.56	2.57	1.02	2.56
		Self-supported steel lattice tower with 9144mm leg extension	34336.2555	1.64	0.60	2.71	2.41	1.01	2.37	2.41	1.01	2.37
		Guyed-V steel lattice tower	15759.55	1.50	0.61	2.47	2.14	0.97	2.20	2.14	0.97	2.20

Table 7.3 Average impact factors for line models with flexible structures (Span Length 214m)

Insulator Length	RTS %	Tower Type	k'	Bare conductor			Half inch ice load			one inch ice load		
				IFI	RR	IFF	IFI	RR	IFF	IFI	RR	IFF
		Basic steel lattice tower	49211	1.65	0.50	3.29	3.01	0.86	3.49	2.10	0.63	3.34
	15	Steel tubular Pole structure	1785.66	1.10	0.43	2.54	1.36	0.70	1.95	1.20	0.52	2.37
		H-frame wood pole structure	1066.25	1.31	0.39	3.35	2.25	0.62	3.61	1.62	0.47	3.40
		Basic steel lattice tower	49211	1.42	0.45	3.17	2.43	0.74	3.30	1.77	0.55	3.21
2.12m	20	Steel tubular Pole structure	1785.66	0.94	0.36	2.60	1.14	0.57	2.01	1.02	0.43	2.43
		H-frame wood pole structure	1066.25	1.40	0.32	4.34	1.95	0.50	3.89	1.61	0.38	4.27
		Basic steel lattice tower	49211	1.27	0.42	3.05	2.04	0.65	3.16	2.97	0.99	3.00
	25	Steel tubular Pole structure	1785.66	0.69	0.32	2.17	1.07	0.48	2.23	1.28	0.71	1.79
		H-frame wood pole structure	1066.25	1.45	0.28	5.25	1.49	0.42	3.55	2.19	0.62	3.50
		Basic steel lattice tower	49211	1.56	0.44	3.57	2.66	0.76	3.50	4.15	1.26	3.30
	15	Steel tubular Pole structure	1785.66	1.46	0.42	3.41	2.02	0.71	2.78	2.73	1.13	2.36
		H-frame wood pole structure	1066.25	1.54	0.39	3.84	3.15	0.65	4.95	4.07	1.04	4.04
		Basic steel lattice tower	49211	1.32	0.38	3.47	1.32	0.38	3.45	3.47	1.03	3.38
3.1m	20	Steel tubular Pole structure	1785.66	1.10	0.36	3.05	1.16	0.37	3.10	2.40	0.91	2.54
		H-frame wood pole structure	1066.25	1.32	0.33	4.06	1.36	0.34	4.06	4.07	0.83	5.10
		Basic steel lattice tower	49211	1.15	0.35	3.33	1.90	0.56	3.40	1.90	0.56	3.40
	25	Steel tubular Pole structure	1785.66	0.97	0.32	2.94	1.39	0.50	2.71	1.39	0.50	2.71
		H-frame wood pole structure	1066.25	1.51	0.29	5.26	1.58	0.45	3.51	1.58	0.45	3.51

8.0 SUMMARY AND CONCLUSIONS

The effects of structure type (self supported lattice tower, Guyed-V steel lattice tower, steel tubular pole structure and H-frame wood pole structure), insulator length, terrain condition, initial conductor tension, and conductor condition were examined for their effect on the impact factors, and maximum transient longitudinal force that was induced on the support structure after conductor rupture. With the limited analytically generated data the following conclusions are inferred:

The structures' flexibility and span/insulator length ratios have a considerable effect on the residual conductor tension, where as peak insulator dynamic tension is affected not only by the supporting structures' flexibility but also by the mass of the cross arm and the type of supporting structure. For stiff structures, the mass has very little effect on the peak insulator tension. For flexible structures it is thought there is a greater ability to transfer potential energy stored in the system as compared to stiff structures. Therefore the peak dynamic loads decrease as flexibility increases. In addition as the amount of stored energy in the system increase due to ice loading or initial stringing tension then the peak dynamic force increases. The higher cross arm mass is thought to increase the peak dynamic load experienced by the system because it is located above the center of gravity of the structure and hence creates a greater moment about the base of the structure.

For transmission lines modeled with stiff supporting structures, the impact factors do not vary much by the varying the support structure stiffness, whereas for lines modeled with flexible structures, like the H-frame, wood pole structure and steel tubular pole structures, the residual force in the conductor depends on both stiffness and span/insulator string length and span/sag ratios.

The following conclusions are arrived from this research

a) There is no appreciable effect of insulator string length on IFI factor The impact factor IFI decreases as initial stringing tension increases

b) The impact factor IFI is not affected appreciably by the type of tower support used in the transmission line model or the type of terrain selected with stiff towers viz., Guyed-V steel lattice tower, self-supported steel lattice towers.

c) The terrain type doesn't influence the impact factors very much for transmission line models that were considered in this analysis. It should be noted each transmission line model is modeled with one type of terrain and one type of tower. The impact factors may be different if the terrain a combination of different terrain.

d) From the parameters used for simulations in this study, the most important design variables that affect the impact factors are the initial stringing tension with bare conductor on the transmission line and conductor condition.

e) The effect of insulator string length has more effect of residual ratio than peak impact factors. For stiff line models generated using stiff structure there is no appreciable effect of type of structure on the impact factors. As the initial conductor tension increases, the impact factors decreases.

f) For line models that generated using flexible structures, the type of tower has more influence on both peak impact factors and residual ratio.

g) The impact factors reduce as the span length decreases.

9.0 RECOMMENDATIONS FOR FUTURE WORK

Based on this study, the following recommendations are given for future work.

1 Anti-cascading structure in the line. To date a study involving simulations has not been performed with a cascade arresting tower in the middle (or somewhere in the middle two thirds) of the transmission line model but rather all have been located at the ends. Expanding the knowledge in this area would be useful for designers as well as transmission line maintenance.

2 Inter-phase spacers and their affect on the damping of a dynamic response. A study has never been performed in this area before and it would be of great benefit to designers to better understand the impact that inter-phase spacers play on the peak dynamic load of a transmission line and their use to damp out forces in a transmission line that are the result of conductor failure and/or component failure.

3 Steep grade of terrains. This study examined low grade slopes which appeared to be negligible in their affect on the response however steeper grades are thought to have a potential to greatly increase the dynamic force in a line and hence needs to be examined in future work. Varying the grades greater than 10% and under 25% would be of use.

4 Different types of insulator strings. This study was narrow in that only two differing length insulators were used, however varying other parameters such as material type, connection point and type, and shape, would be of benefit.

5 Ice shedding on conductors. This needs to be explored further as research in this area to date is minimal but yet this is a very common phenomenon in industry.

6 Wind load and ice load on both towers and conductors. Research in these areas is increasing but exclusive of one another to date and hence has yet to provide the overall picture. Since this phenomena occurs simultaneously in many regions this needs to be studied in the future.

References

1. Tucker, K. B. and Haldar, A., (2006) "Numerical Model Validation and Sensitivity Study of a Transmission Line Insulator Failure Using Full Scale Test Data", IEEE Transactions on Power Delivery, vol. 22, No. 4, October 2007, 2439-2445.

2. Haro, L., Magnusson, B. and Ponni, K., (1956) "Investigation of Forces Acting on A Support After Conductor Breakage", Paper No. 210, International Conference on Large Electric Systems (CIGRE), Paris, 15 pages.

3. Lummis, J., Fiss, R.A., (1969) "Effect of Conductor Imbalance on Flexible Transmission Structures" IEEE Transactions on Power Apparatus and Systems, Vol. PAS-88, No. 11, November 1969, pp1672-1678.

4. Govers, A., (1970) "On The Impact of Unidirectional Forces on High Voltage Towers Following Conductor Breakage", Paper No. 22-03, International Conference on Large Electric Systems, 10 pages.

5. Peyrot, Alain H., Kluge, Robert O., and Lee, Jun W., (1978) "Longitudinal Loading Tests on a Transmission Line", EL-905, September, 145 pages.

6. Lindsey, K.E. (1978a). "Mathematical Theory of Longitudinally Loaded Elastic-Plastic transmission Lines-statics." IEEE Transactions on Power Apparatus and Systems, PAS-97(2), 574-582.

7. Mozer, J. D., Wood, W. A. and Haribor, J. A., (1981) "Broken Wire Tests on a Model Transmission Line System", IEEE Transactions on Power Apparatus and Systems, PAS-100: pp. 938 - 947.

8. Thomas, M. B., and Peyrot, A. H., (1982) "Dynamic Response of Ruptured Conductors in Transmission Lines", IEEE PES, Winter Meeting, pp. 1 - 5.

9. Richardson, A.S. (1987) "Longitudinal Dynamic Loading of a Steel Pole Transmission Line" IEEE Transactions on Power delivery, PERD-2(2), 425-436.

10. McClure, G. and Tinawi, R., (1987) "Mathematical Modeling of the Transient Response of Electric Transmission Lines Due to Conductor Breakage", Computers and Structures, Vol 26, No. ½, pp. 41-56.

11. Jamaleddine, A., McClure, G., Roousselet, J., and Beauchemin, R. (1993). "Simulation of Ice Shedding on Electrical Transmission Lines Using ADINA." Computers and Structures, 47(4/5), 523-536.

12. Gupta, S., Wipf, T.J., Fanous, F., Baenziger, M., and Hahm, Y.H. (1993) 'Structural Failure Analysis of 345 kV Transmission." IEEE PES Summer Meeting, Vancouver, BC, Paper No. 93 SM 441-6 PWRD.

13. Ostendorp, M. (1997a-d) Longitudinal Load and Cascading failure Risk Assessment (CASE) Volume 1: Simplified Approach. TR-107087-V1, Electric Power Research Institute, Palo Alto, CA.

14. Kempner, L. J., (1997) "Longitudinal Impact Loading on Electrical Transmission Line Towers: A Scale Model Study", PhD Thesis, System Science: Civil Engineering, Portland State University, Portland, Oregon, 201 pages.

15. Fekr, M.R., McClure, G., (1998) "Numerical Modeling of the Dynamic response of Ice-shedding on Electrical Transmission Lines" Atmospheric Research, 46, 1998, 1-11.

16. Peabody, A.B., and McClure, G., (2002) "Load Limiters for Overhead Lines", 4th Structural speciality conference of the Canadian Society for Civil Engineering, June 2002.

17. McClure, G., and Lapointe, M. (2003) "Modeling the Structural Dynamic Response of Overhead Transmission Lines." Computers and Structures, 81, 825-834.

Bibliography

1 Brown, R.S. (1913). "Stresses Produced in a Transmission Line by Breaking of a Conductor." Electrical world, March 29, 1913, 673-676.

2 Buchanan, W.B. (1934). "Vibration Analysis-Transmission Line Conductors." Transactions of the AIEE, 53, 1478-1485.

3 Bissiri, A., and Landau, M. (1947). "Broken Conductor effect on Sags in Suspension Spans." AIEE Transactions, 66, 1181-1188.

4 Elgerd, O. I. (1963) "Transient Suspension Forces caused by Broken Transmission Line Conductors." Journal of the Franklin Institute, 275(3), 227-245.

5 Bonar, P.P. (1968) " Dynamic Testing of Lattice Steel Masts." International Conference on Large High Tension electric Systems (CIGRE), Paris, Paper 22-04.

6 Campbell, D.B. (1970). "Unbalanced Tensions in Transmission Lines" Journal of the Structural Division, ASCE, 96(ST 10), 2189-2207.

7 Peyrot, A.H., and Goulois, A.M. (1978) "Analysis of Flexible Transmission Lines" Journal of the Structural Division, ASCE, 104(ST5), 763-779.

8 Thomas, M. B., (1981) "Broken Conductor Loads on Transmission Line Structures", PhD Thesis, University of Wisconsin, Madison, 311 pages.

9 Siddiqui, F., and Fleming, J., (1984) "Broken Wire Analysis of a Transmission Line Systems", Computers and Structures, Vol 18, No. 6, pp. 1077-1085.

10 Anjam, R. (1991). Galloping and Broken Conductor Analysis of Transmission Lines, M.S. Thesis, Civil and Construction Engineering, Iowa State University, Ames, Iowa.

11 Gupta, S. (1991). Nonlinear Analysis of transmission Line Structures Subjected to Ice Loads, M.S. Thesis, Civil and Construction Engineering, Iowa State University, AMES, Iowa.

12 Roshan, Fekr, M. (1995). Dynamic Response of Overhead Transmission Lines to Ice Shedding, M.Eng. Thesis, Civil engineering and Applied mechanics, McGill University, Montreal, Quebec.

13 Commission – 1998 Ice Storm. (1999a) Facing the Unforeseeable, Lessons from the Ice storm of '98, Les Publications du Quebec, Quebec.

14 Commission – 1998 Ice Storm. (1999b) La Securite Civile (Public Safety): Rapport de la Commission Scientifique et Technique Chargee D'analyser les Evenements Relatifs a la Tempete de Verglas Survenue du 5 au 9 Janvier 1998, Les Publications du Quebec, Quebec.

15 Commission – 1998 Ice Storm. (1999c) La Securite Civile (Public Safety): Rapport de la Commission Scientifique et Technique Chargee D'analyser les Evenements Relatifs a la Tempete de Verglas Survenue du 5 au 9 Janvier 1998, Les Publications du Quebec, Quebec.

16 Commission – 1998 Ice Storm. (1999d) La Securite Civile (Public Safety): Rapport de la Commission Scientifique et Technique Chargee D'analyser les Evenements Relatifs a la Tempete de Verglas Survenue du 5 au 9 Janvier 1998, Les Publications du Quebec, Quebec.

17 Commission – 1998 Ice Storm. (1999e) La Securite Civile (Public Safety): Rapport de la Commission Scientifique et Technique Chargee D'analyser les Evenements Relatifs a la Tempete de Verglas Survenue du 5 au 9 Janvier 1998, Les Publications du Quebec, Quebec.

18 Fleming, J.F., Atkins, S.R., and Mozer, J.D. (1978) "A Program for Longitudinal Load Analysis of Electrical Transmission Lines." Computers and Structures, Sept. 1978, 237-253.

19 Peabody, A.B. (2001). Transmission Line Longitudinal loads, A Review of design Philosophy, Structural engineering Series No. 2001-02, Department of Civil Engineering and Applied Mechanics, McGill University, Montreal.

20 Han, S.W., Cho, H.G., Woo, B.C., Han, D.H., Lee, D.I., choie, I.H., shin, T.W., (2003) "Simulation on Interface mechanical Stress in Porcelain Insulators for Transmission Line by Cement Growth Using ANSYS/NASTRAN Program" Proceedings of the 7th International Conference on Properties and Application of Dielectric Materials, June I-5, 2003.

21 Lapointe, Marc, (2003) "Dynamic Analysis of Power Line Subjected to Longitudinal Loads", Master of Engineering Thesis, McGill University, Montreal, 105 pages.

22 ADINA (Automatic Dynamic Incremental Nonlinear Analysis), (2003). Version 8.6. ADINA R&D, Watertown, MA.

23 Munaswamy, K., Haldar, A., (2000) "Self-damping Measurements of Conductors with Circular and Trapezoidal Wires", IEEE Transactions on Power Delivery, Vol. 15, No. 2, April, pp 604-609.

24 Ferry-Borges, F. (1968) "Experimental Study of the Stresses Created by the Breakage of Conducctors in High-Voltage Lines" Department of Public Works, National Civil Engineering Laboratory, Lisbon, Portugal, November, 1968.